

The Observed Luminosity Correlations of Gamma-Ray Bursts and Their Applications

Chen Deng ¹ , Yong-Feng Huang ^{1,2,*} , Fan Xu ³  and Abdusattar Kurban ^{4,5,6} 

¹ School of Astronomy and Space Science, Nanjing University, Nanjing 210023, China

² Key Laboratory of Modern Astronomy and Astrophysics (Nanjing University), Ministry of Education, China

³ Department of Physics, Anhui Normal University, Wuhu 241002, China

⁴ Xinjiang Astronomical Observatory, Chinese Academy of Sciences, Urumqi 830011, Xinjiang, China

⁵ Key Laboratory of Radio Astronomy and Technology (Chinese Academy of Sciences), Beijing 100101, China

⁶ Xinjiang Key Laboratory of Radio Astrophysics, Urumqi 830011, Xinjiang, China

* Correspondence: hyf@nju.edu.cn

Abstract: Gamma-ray bursts (GRBs) are among the most luminous electromagnetic transients in the universe, providing unique insights into extreme astrophysical processes and serving as promising probes for cosmology. Unlike Type Ia supernovae, which have a unified explosion mechanism, GRBs cannot directly act as standard candles for tracing cosmic evolution at high redshifts due to significant uncertainties in their underlying physical origins. Empirical correlations derived from statistical analyses involving various GRB parameters provide valuable information regarding their intrinsic properties. In this brief review, we describe various correlations among GRB parameters involving the prompt and afterglow phases, discussing possible theoretical interpretations behind them. The scarcity of low-redshift GRBs poses a major obstacle to the application of GRB empirical correlations in cosmology, referred to as the circularity problem. We present various efforts aiming at calibrating GRBs to address this challenge and leveraging established empirical correlations to constrain cosmological parameters. The pivotal role of GRB sample quality in advancing cosmological research is underscored. Some correlations that could potentially be utilized as redshift indicators are also introduced.

Keywords: gamma ray bursts; observational relationships; cosmological parameters; redshift indicators

1. Introduction

Gamma-ray bursts (GRBs) are one of the most energetic stellar explosion events in the universe, with the isotropic equivalent energies ranging from $10^{48} - 10^{55}$ erg [1–6]. Since their discovery in the 1960s, the use of various observational instruments has led to groundbreaking advancements in the field of GRBs, significantly deepening our understanding of their physical nature [7–13]. The Burst and Transient Source Experiment (BATSE) on board the Compton Gamma Ray Observatory (CGRO) revealed an isotropic spatial distribution of GRBs, suggesting their cosmological origin [14–18]. This was unequivocally confirmed by the detection of the multi-wavelength afterglow of GRB 970508, leading to the first redshift measurement of $z = 0.835$ for it [19].

Observationally, the duration of GRBs' prompt emission, represented by T_{90} , is defined as the time interval during which 5%–95% of gamma-ray photons are detected. This duration exhibits a bimodal distribution, with approximately 2 seconds as the dividing line [20]. Long GRBs (LGRBs, $T_{90} > 2$ s) are found in star-forming galaxies and are associated with Type Ic supernovae [21–31]. This indicates that LGRBs originate from the collapse of massive stars, with Wolf-Rayet stars as the likely progenitors [32–37]. On average, short GRBs (SGRBs, $T_{90} < 2$ s) display a larger offset relative to their host galaxies compared to LGRBs [38–41]. Additionally, their optical/infrared afterglows may contain a kilonova component,

Citation: Deng C.; Huang Y.-F.; Xu F.; Kurban A. GRB correlations. *Journal Not Specified* **2024**, *1*, 0.
<https://doi.org/>

Received:

Revised:

Accepted:

Published:

Copyright: © 2025 by the authors. Submitted to *Journal Not Specified* for possible open access publication under the terms and conditions of the Creative Commons Attribution (CC BY) license (<https://creativecommons.org/licenses/by/4.0/>).

as predicted by the merger of neutron star - neutron star (NS-NS) binaries or neutron star - black hole (NS-BH) binaries [42–49]. The association of GRB 170817A with the gravitational wave event GW170817 detected by the advanced Laser Interferometer Gravitational Wave Observatory provides strongly evidence that binary neutron star mergers are one of the progenitors of SGRBs [50–52]. Interestingly, some GRBs exhibit characteristics of both long and short GRBs. For example, GRB 211211A, though classified as a LGRB, is associated with a kilonova – a phenomenon typically linked to SGRBs [47,48,53]. The classification of GRBs solely based on their duration may lead to confusion. This is because the prompt emission duration is energy and sensitivity dependent, meaning that the duration may vary across different detectors [54]. The overlap in the duration distributions of long and short GRBs suggests the possible existence of an intermediate-duration group [55–58]. Furthermore, the discovery of some subclasses, such as SGRBs with extended emission and ultra-long GRBs, has introduced challenges to the traditional GRB classification [59–63]. To address these complexities, machine learning methods have been applied to enhance GRB classification [64,65]. In addition, Zhang et al. [66,67] proposed a physical classification system that divides GRBs into Type I and Type II by integrating multiple criteria, including spectral information, empirical correlations, host galaxy characteristics, and associations with supernova or kilonova.

A GRB generally consists of two phases: the prompt emission phase and the afterglow phase. The prompt emission phase can last from sub-seconds to thousands of seconds [68], with light curves that exhibit highly irregular and rapid variations [8]. This phase may also contain multiple emission episodes [69–71], which includes quiescent stages in which the flux drops to nearly background level. The pulse profiles of the prompt emission generally display an asymmetric shape, commonly described by a “fast-rise exponential decay” (FRED) pattern [72,73]. The prompt emission spectrum of GRBs can be phenomenologically characterized by the so-called Band function [74], with typical photon spectral indices of -1 and -2 for the low-energy and high-energy segments [75], respectively. In addition, some GRBs show thermal or high-energy components in their prompt phase [76–83]. The spectral evolution of GRBs usually follows two patterns [84–86]: one is the “hard-to-soft” pattern, where the peak photons gradually shifts from high to low energies, and the other is the “flux-tracking” pattern, in which the spectral evolution synchronizes with the flux variations. In some GRBs, a transition between these spectral evolution modes can occur [87], further highlighting the diversity and complexity of GRB radiation processes. Following the prompt emission, the afterglow phase ensues, which can last for months or even longer. The multi-wavelength afterglow emission covers the entire electromagnetic spectrum, and the afterglow light curves are typically smoother than those of the prompt phase, often described by a multi-segment power-law function. Thanks to the *Swift* satellite’s rapid slewing capability, some elusive components in early X-ray afterglows have been revealed [88–90]. With the accumulation of the observational data, Zhang et al. [91] summarized a canonical X-ray light curve with five components, noting that GRBs may exhibit some or even all of these features. Additionally, an analogous hypothetical optical light curve with richer features has also been proposed [92].

The so called “fireball” model has been established for GRBs to explain the rich observational phenomena in both the prompt and afterglow phases [93–95]. Following the catastrophic destruction of the progenitor star, a hyper-accreting black hole or highly magnetized neutron star is left, which could act as the central engine of a GRB [96–99]. The central engine launches a series of ultra-relativistic shells with different speed. These shells collide at distances of approximately 10^{14} to 10^{16} cm from the central engine, generating internal shocks that accelerate electrons to produce optically thin synchrotron radiation [100–103]. Additionally, the photosphere model, another explanation for the prompt emission, has also been widely discussed. When additional effects are considered, this model can also account for non-thermal spectrum observed in some GRBs [104,105]. As the merged shells sweep up the surrounding medium, external forward shocks are formed, leading to the production of multi-wavelength afterglows, spanning from radio waves to gamma

rays [106]. However, despite the wide acceptance of the fireball model, our understanding of the physical mechanisms underlying GRBs, particularly during the prompt emission phase, remains limited. Synchrotron radiation and synchrotron self-Compton scattering can account for some spectral features of GRBs, which predict that the low-energy spectral index should not exceed $-2/3$, a threshold known as the synchrotron “line of death” [107]. Nevertheless, in some GRBs, the spectral index α does exceed $-2/3$, suggesting that the prompt emission likely arises from a combination of multiple, complex radiation processes [108,109]. The fireball dynamics is well described by the Blandford-McKee self-similar solution [110], which, combined with the slow-cooling synchrotron radiation mechanism, can effectively explain the power-law decay behavior of the observed X-ray afterglow. However, the X-ray/internal plateaus seen in some afterglows deviate from the predictions of the standard forward shock model. To address this discrepancy, researchers have proposed several models to explain the plateau phase [96,111–114].

Since GRBs are extremely luminous, they can be detected at high redshifts. The highest redshift record of detected GRBs is 9.4 [115,116]. So, GRBs can be potentially used as robust cosmological probes. GRBs offer a unique opportunity to investigate the history of star formation, metal enrichment, and cosmic reionization at high redshift (see Ref. [117] and references therein). However, unlike Type Ia supernovae (SNe Ia), which have a uniform explosion mechanism, the physical processes behind GRBs are not fully understood. Additionally, the isotropic energy of GRBs spans several orders of magnitude, making it challenging to directly use them as standard candles to explore the high-redshift universe. In this context, identifying universal observational correlations that can standardize GRBs becomes particularly important. These empirical correlations offer critical insights into GRB classification, the emission mechanisms, and the structure and evolution of GRB jets. Here we present a review on various aspects of GRBs, paying special attention on the correlations involving their luminosity.

This article is organized as follows. In Section 2, we provide a brief overview of the discovery and development of some empirical correlations concerning the parameters of the prompt phase and afterglow phase, and discuss possible physical interpretations underlying these correlations. Section 3 presents the application of some empirical correlations in constraining cosmological parameters. The usage of some correlations as pseudo-redshift indicators is also described. Finally, Section 4 presents our conclusions.

2. GRB Prompt and Afterglow Correlations

This section provides a brief summary of common empirical correlations related to GRB prompt and afterglow parameters, followed by a discussion of their potential physical origins. For comprehensive reviews on GRB prompt and afterglow correlations, the readers could refer to Refs. [118–121].

2.1. GRB prompt correlations

2.1.1. The $L_p - \tau_{\text{lag}}$ correlation

Norris et al. [122] first identified an inverse correlation between the peak luminosity (L_p) and spectral lag (τ_{lag}) based on a sample of six BATSE GRBs with known redshifts, described as

$$\frac{L_p}{10^{53} \text{erg s}^{-1}} = 1.3 \left(\frac{\tau_{\text{lag}}}{0.01 \text{ s}} \right)^{-1.14}, \quad (1)$$

where L_p denotes the isotropic equivalent peak luminosity in 50 – 300 keV and τ_{lag} is defined as the delay between BATSE channels 1 and 3, which correspond to the energy ranges of 25-50 keV and 50-300 keV, respectively. This finding is confirmed by the analysis results reported by Schaefer et al. [123], who calculated the peak flux using 256 ms time bin for 50–300keV, based on 112 BATSE GRBs with no measured redshifts. Tsutsui et al. [124] investigated the $L_p - \tau_{\text{lag}}$ correlation with pseudo-redshifts derived from the Yonetoku

relation for 565 BATSE GRBs, noting a substantial dispersion with a correlation coefficient of only 0.38. Furthermore, a redshift-dependent $L_p - \tau_{\text{lag}}$ correlation was proposed as

$$\frac{L_p}{10^{52} \text{erg s}^{-1}} = 10^{-1.12 \pm 0.07} (1+z)^{2.53 \pm 0.10} \tau_{\text{lag}}^{-0.28 \pm 0.03}. \quad (2)$$

In contrast to the spectral lag extracted from different energy channels in the observer frame, Ukwatta et al. [125] analyzed a sample of 43 *Swift* GRBs with known redshifts to update the luminosity-lag correlation in the GRB source frame. Their result is characterized by a power-law index of -1.2, i.e., $L_p \propto (\tau_{\text{lag}}/(1+z))^{-1.2 \pm 0.2}$. The energy channels used to compute the spectral lag in their study are 100-150 keV and 200-250 keV for *Swift* BAT in the GRB rest frame. In addition, similar luminosity-lag relation was also revealed in X-ray flares of GRB afterglows [126], suggesting that they may share the same radiation mechanism as the prompt emission.

From a physical perspective, Salmonson et al. [127] proposed that the $L_p - \tau_{\text{lag}}$ correlation is purely a kinematic effect, where the peak luminosity is proportional to the Lorentz factor Γ of the jet shell, and the lag time is inversely proportional to Γ . In this model, the luminosity in the comoving frame of GRB emission region remains nearly constant, while the apparent luminosity measured by the observer is determined entirely by the Lorentz factor along the line of sight. Consequently, the Lorentz factor and the observed luminosity must vary within the same order of magnitude. This clearly does not align with the case of GRBs, since the variation in peak luminosity far exceeds the range of Lorentz factor variation derived from the afterglow data [128–130].

Schaefer [128] suggested that the lag time partially reflects the pulse cooling process. In high-luminosity GRBs, the cooling time is brief, resulting in a shorter lag, whereas the cooling time of low-luminosity GRBs is longer, leading to an extended lag. In the context of internal shocks, Ioka et al. [131] attributed the variations in luminosity and spectral lag across different GRBs to the observer's viewing angle. GRBs with high luminosity and short lag are observed at smaller viewing angles, while low-luminosity GRBs with longer lag are associated with larger viewing angles. This interpretation also offers insight into the $L - V$ correlation. Additionally, the curvature effect may also contribute to the observed spectral lag [132,133].

2.1.2. The $L_p - V$ correlation

Reichart et al. [134] analyzed a sample of 20 GRBs with known redshifts. They found a positive correlation between the peak luminosity (L_p) and time variability (V), i.e.,

$$L_p \propto V^{3.3_{-0.9}^{+1.1}}. \quad (3)$$

This correlation is consistent with the results reported by Fenimore et al. [135], though the definition of V varies slightly between the two studies. Guidorzi et al. [136] reanalyzed the $L_p - V$ correlation using a larger sample of 32 GRBs. While the correlation still holds, the power-law index differs significantly from previous one. Reichart et al. [137] argued that this discrepancy stemmed from the use of improper statistical methods. They updated the index as 3.4, which is consistent with earlier findings.

Different analysis method and different definition of variability can result in various slopes in the $L_p - V$ correlation [138–140]. With a substantial increase in sample size, Guidorzi et al. [141] observed that the $L_p - V$ correlation became so scattered that it was challenging to establish a clear relationship. Nevertheless, an inverse correlation between the peak luminosity and the minimum variability timescale was identified [142], despite the significant dispersion.

In the context of internal shocks, the observed $L - V$ relationship may arise from the dynamics of relativistic jets in GRBs [143]. Both luminosity and variability are governed by the Lorentz factor of the jet shell. Owing to relativistic beaming effects, the size of the radiation region observed by a distant observer is inversely proportional to the Lorentz

factor of the jet. Consequently, GRBs with higher Lorentz factors exhibit greater luminosity and a smaller emission region, resulting in increased variability.

This correlation may also be influenced by the opening angle of the jet [144,145]. It is argued that jets with a smaller opening angle exhibit lower baryon loading, potentially leading to a higher Lorentz factor. Furthermore, the photospheric effect could play a role in the $L - V$ correlation [141,145,146]. In GRBs with a lower Lorentz factor, the internal shock radius of the shell will be small and may lie below the photospheric radius. This would smooth the pulse profile of the prompt emission, thereby reducing the variability. Salafia et al. [147] proposed that the off-axis effect can significantly broaden the prompt pulse, smearing out the light curve variability.

2.1.3. The $E_p - E_{\text{iso}}$ correlation

The $E_p - E_{\text{iso}}$ correlation, commonly known as the Amati relation, is among the most discussed empirical correlations in GRB studies. It was first introduced by Amati et al. in analyzing 12 BeppoSAX GRBs with known redshifts [148], which is expressed as

$$E_p \propto E_{\text{iso}}^{0.52 \pm 0.06}. \quad (4)$$

Here, the peak energy E_p is derived by fitting the time-integrated spectrum using the Band function [74], while the isotropic equivalent energy E_{iso} represents the total energy within the $1 - 10^4$ keV range. It was further confirmed that X-ray rich GRBs (XRRs) and X-ray flashes (XRFs) also follow the same Amati relation as classical LGRBs [149,150].

Later, Amati et al. [151] analyzed an expanded sample of 70 GRBs and XRFs, and confirmed that the Amati relation remains valid, with a slope consistent with previous findings. With increasing sample sizes and improved data quality, researchers have conducted more comprehensive studies of the Amati relation [152–155]. It is found that although the derived slopes vary slightly, they generally cluster around 0.5.

Although SGRBs do not adhere to the Amati relation established for traditional LGRBs and XRFs, they occupy a parallel region in the $E_p - E_{\text{iso}}$ plane [152]. This indicates that, on average, SGRBs exhibit lower isotropic equivalent energy at similar peak energies compared to LGRBs [124].

Nava et al. [156] analyzed the Amati relation based on *Swift* GRBs across different redshift bins. They found that the slope of the correlation does not evolve with redshift. Demianski et al. [155] parameterized the redshift evolution of the observables in the Amati relation and confirmed the absence of redshift evolution in this relation. Furthermore, a similar relation has also been found to exist inside each GRB based on time-resolved spectral analysis, with both the slope and normalization being similar to those derived from time-integrated spectrum [157,158].

Despite extensive discussions regarding the Amati relation since its discovery, the physical mechanism responsible for this correlation remains poorly understood. This limited understanding is largely due to our incomplete knowledge of the radiation mechanisms driving prompt GRB emission, the processes involved in electron acceleration by internal shocks, and the amplification of magnetic fields in the radiation region [121]. Photospheric emission is a natural prediction of the standard fireball model for GRBs and may influence the prompt emission spectrum [159–162]. Thompson et al. [159] interpreted the thermally peaked emission, Doppler boosted by the GRB outflow, as the peak energy, while the non-thermal high-energy emission arises from inverse Compton scattering by the relativistic electrons outside the photosphere. This model predicts a power-law index of 0.5 for the Amati relation.

Eichler & Levinson [163] proposed that a ring-shaped fireball with viewing angle effects could reproduce the Amati relation, with a power-law index of 0.5. Without specifying radiation processes, Dado et al. [164] suggested that the Amati relation may have a dynamical origin and they derived a slope of 0.5 based on the so-called cannonball model. Additionally, several authors have attempted to reproduce the Amati relation through numerical simulations [165–167]. Mochkovitch et al. [167] demonstrated that the internal

shock model can explain the observations. They further provided strict constraints on the dynamics and the microphysical parameters governing shock energy dissipation.

Some GRBs deviate significantly from the Amati relation, indicating that they could be off-axis events [168–171]. Xu et al. [172] analytically derived the on-axis and off-axis Amati and Yonetoku relations (also see Section 2.1.4) within the framework of the standard fireball model, based on the optically thin synchrotron radiation mechanism under the fast cooling scenario. In the on-axis cases, the Amati relation follows $E_p \propto E_{\text{iso}}^{0.5}$, whereas in the off-axis cases, this correlation is modified to $E_p \propto E_{\text{iso}}^{1/4 \sim 4/13}$, where the range reflects variations in the viewing angle beyond the jet core.

2.1.4. The $E_p - L_p$ correlation

Yonetoku et al. [173] found a positive correlation between E_p and L_p , known as the Yonetoku relation, which is expressed as

$$\frac{L_p}{10^{52} \text{ erg s}^{-1}} = \left(2.34_{-1.7\%}^{+2.29}\right) \times 10^{-5} \left[\frac{E_p(1+z)}{1 \text{ keV}}\right]^{2.0 \pm 0.2}, \quad (5)$$

where the peak energy E_p is derived from the Band function [74], and the peak luminosity L_p is the 1-second peak luminosity. Using this relation, Yonetoku et al. [173] calculated the pseudo-redshifts of 689 BATSE GRBs and argued that there is redshift evolution in the relation.

Further research by Ghirlanda et al. [174] revealed that BATSE SGRBs without measured redshifts adhere to the Yonetoku relation but deviate from the Amati relation. If SGRBs follow the Yonetoku relation of LGRBs, their pseudo-redshift distribution resembles that of LGRBs, albeit with a lower average redshift. The validity of the Yonetoku relation in SGRBs with confirmed redshifts has been verified by a number of studies [175–180]. In the $E_p - L_p$ plane, SGRBs are dimmer by a factor of approximately 5 compared to LGRBs with same E_p [180]. Some low-luminosity GRBs clearly deviate from the Yonetoku relation, suggesting an origin possibly different from that of classical LGRBs [181].

Yonetoku et al. [181] utilized an expanded sample consisting of 101 GRBs with well-defined spectral information to update the Yonetoku relation as

$$L_p = 10^{52.43 \pm 0.037} \times \left[\frac{E_p(1+z)}{355 \text{ keV}}\right]^{1.60 \pm 0.082}, \quad (6)$$

where the slope of the updated relation is slightly smaller than the original one but remains consistent at the 2σ confidence level.

Some authors have argued that the Yonetoku and Amati relations could be significantly impacted by detector threshold truncation effects [182–184], casting doubts on their authenticity. However, subsequent detailed analyses indicated that both relations are intrinsic [181]. The Yonetoku relation shows slight redshift evolution, whereas the Amati relation is modestly affected by detector threshold effects, which may contribute to the observed dispersion in the Amati relation. Yonetoku et al. [173] proposed that the redshift dependence observed in the peak luminosity could arise from the evolution of GRB progenitors or jet opening angles with redshift.

According to the standard fireball model with synchrotron radiation [172], the on-axis Yonetoku relation can be derived analytically as $E_p \propto L_p^{0.5}$, in which the power-law index is largely consistent with the observations. In the off-axis cases, the Yonetoku relation is modified to $E_p \propto L_p^{1/6 \sim 4/17}$, where the power-law index is flatter than that of the Amati relation. The outliers of the Amati and Yonetoku relations could stem from viewing angle effect. Interestingly, they are more easily identifiable in the Yonetoku relation than in the Amati relation.

While the optically thin synchrotron radiation model can effectively account for the spectral-luminosity (or energy) correlations, its simplified parameterization and significant uncertainties in various physical parameters limit the predictive power over emission

properties. Consequently, the photosphere model, based on thermal radiation, has gained favor among some researchers and has been applied to explain the Yonetoku relation [162,185–188]. Ito et al. [189] conducted three-dimensional hydrodynamic simulations, demonstrating that the Yonetoku relation naturally arises from viewing angle effects. The dispersion in the Yonetoku relation may stem from the intrinsic properties of GRB jets, such as the jet power, Lorentz factor, and duration.

2.2. prompt and afterglow correlations

2.2.1. The $L_X - T_a$ correlation

Dainotti et al. [190] analyzed 33 LGRBs and discovered an anti-correlation involving the X-ray afterglow plateau of GRBs, known as the Dainotti relation, which has the following form,

$$\log L_X = a + b \log T_a, \quad (7)$$

where T_a represents the end time of the plateau phase in the GRB rest frame (in seconds), and L_X is the corresponding X-ray luminosity at T_a (in erg s^{-1}). The K -correction accounting for the cosmic expansion is applied in calculating the X-ray luminosity [191]. The afterglow light curve is described using a phenomenological two-component model [192]. The normalization constant a and slope b in the original version are 48.54 and $-0.74^{+0.20}_{-0.19}$, respectively. Subsequently, Dainotti et al. [193] employed an expanded sample of 62 LGRBs to update the Dainotti relation as $L_X \propto T_a^{-1.06^{+0.27}_{-0.28}}$. This relation also holds for intermediate-duration GRBs, albeit with a steeper slope. The Dainotti relation remains valid for larger samples, and although the slopes reported in various studies may differ slightly, they are largely consistent. [193–200].

The varying slopes derived from different samples may be influenced by redshift evolution and selection bias, which could undermine the robustness of the correlation as a cosmological probe. Dainotti et al. [198] applied the Efron & Petrosian (EP) method [201] to correct for the redshift evolution of L_X and T_a . Using a sample of 101 GRBs with well-defined light curves, they demonstrated that the $L_X - T_a$ correlation is intrinsic for a significant portion of GRBs, with a slope of -1.07 . Moreover, similar 2D Dainotti relation has been investigated in the optical and radio bands [202,203].

Dainotti et al. [200] identified a significant difference in the Dainotti relation among subsamples of LGRBs with and without supernovae. This difference persisted even after applying the EP method to correct for the redshift evolution in LGRBs without supernovae.

Additionally, Dainotti et al. [204] combined the $L_X - T_a$ correlation with the L_p of the GRB prompt phase to derive a new three-parameter relation, denoted as

$$\log L_X = (15.75 \pm 5.3) - (0.77 \pm 0.1) \log T_a + (0.67 \pm 0.1) \log L_p. \quad (8)$$

Following the convention of Dainotti et al. [204,205], we refer to the $L_X - T_a - L_p$ correlation as the 3D Dainotti relation. Dainotti et al. [204] focused on GRBs with sufficient data points in the plateau phase to accurately describe their light curves, designating them as the “gold” sample. The intrinsic dispersion of the 3D Dainotti relation derived based on the gold sample is $\sigma_{\text{int}} = 0.27 \pm 0.04$, significantly smaller than that of the original 2D Dainotti relation. Further study has demonstrated that the 3D Dainotti relation applies to all classes of GRBs, with the intrinsic dispersion reduced to $\sigma_{\text{int}} = 0.22 \pm 0.1$ when using platinum sample selected under stringent criteria [206].

The X-ray plateau phase is not a phenomenon predicted by the traditional forward shock model [91]. It may be linked to the reactivation of the central engine or reflect the angular structure of the GRB jet [147,207,208], both of which are crucial for understanding the nature of GRBs.

In a framework involving a black hole with fallback accretion, Cannizzo et al. [209] proposed that the Dainotti relation can be reproduced if the accreted matter has a unified mass. The power-law index in the Dainotti relation is approximately -1 , indicating that a

constant energy reservoir may be involved in the plateau phase. A plausible explanation is that the central engine of the GRB is not a black hole, but a millisecond magnetar [97,210–212], whose spin-down energy is injected into the external forward shock, producing the observed X-ray plateau. Rowlinson et al. [213] derived a scaling relationship between the plateau luminosity and its duration under the magnetar energy injection scenario, i.e.,

$$\log L_X \sim \log(10^{52} I_{45}^{-1} P_{0,-3}^{-2}) - \log T_a, \quad (9)$$

where I_{45} is the moment of inertia of the magnetar in units of 10^{45} g cm^2 and $P_{0,-3}$ represents the initial spin period of the magnetar in units of millisecond. This is consistent with the anti-correlation identified by Dainotti et al. [198], i.e., $L_X \propto T_a^{-1}$. Variations in the initial spin period of the magnetar may contribute to the dispersion observed in the Dainotti relation. However, while the energy injection scenario often predicts achromatic brightening across multiple bands [214], the expected brightening is not observed in the afterglow light curves in other bands.

An alternative explanation is that the GRB jets may possess angular structures rather than the simplified top-hat shape with sharp edges [114,147,215–217]. The shallow decay phase can naturally result from off-axis observations of forward shock radiation emitted by structured jets propagating through the circumburst medium [215]. This model has the advantage of not requiring long-term central engine activities and can produce plateaus lasting for 10^2 to 10^5 seconds within the appropriate parameter space, in both interstellar medium and wind environments.

2.2.2. The $L_X - T_a - E_{\text{iso}}$ correlation

Xu & Huang [218] collected 77 GRBs that exhibited plateaus in their X-ray afterglows and introduced the E_{iso} of the prompt phase as the third parameter. They derived a tight three-parameter correlation, i.e., the $L_X - T_a - E_{\text{iso}}$ correlation, as,

$$\log\left(\frac{L_X}{10^{47} \text{ erg s}^{-1}}\right) = a + b \times \log\left(\frac{T_a}{10^3 \text{ s}}\right) + c \times \log\left(\frac{E_{\text{iso}}}{10^{53} \text{ erg}}\right), \quad (10)$$

where a , b , and c are coefficient obtained by fitting the observational data. The K -correlation is also considered in the calculation of E_{iso} . The best fitting results derived from the so-called Markov-chain Monte Carlo (MCMC) techniques are $a = 0.81 \pm 0.07$, $b = -0.91 \pm 0.09$, $c = 0.59 \pm 0.05$, and $\sigma_{\text{int}} = 1.15 \pm 0.12$, where σ_{int} represents the intrinsic dispersion of the correlation. A smaller σ_{int} indicates a tighter correlation. After applying additional selection criteria, Xu & Huang [218] defined a golden sample consisting of 47 LGRBs and 8 intermediate-duration GRBs. The best fitting results for this refined sample are $a = 1.17 \pm 0.09$, $b = -0.87 \pm 0.09$, $c = 0.88 \pm 0.08$, and $\sigma_{\text{int}} = 0.43 \pm 0.05$. Evidently, after rigorous sample selection, the intrinsic dispersion is significantly reduced, leading to a tighter $L_X - T_a - E_{\text{iso}}$ correlation.

Tang et al. [219] analyzed a larger sample of 174 plateau GRBs with well-defined light curves and known redshifts. They confirmed the existence of the $L_X - T_a - E_{\text{iso}}$ correlation and updated it as $L_X \propto T_a^{-1.01 \pm 0.05} E_{\text{iso}}^{0.84 \pm 0.04}$. It should be noted that Tang et al. [219] employed a smooth broken power-law function to fit the afterglow light curve, whereas Dainotti et al. [190] used a two-component phenomenological model proposed by Willingale et al. [192]. The difference in the method may lead to slight discrepancies in the fitted plateau duration and the corresponding X-ray luminosity. Deng et al. [220] expanded the sample of Tang et al. [219] with additional 36 plateau GRBs, updating the $L_X - T_a - E_{\text{iso}}$ correlation as $L_X \propto T_a^{-0.99 \pm 0.04} E_{\text{iso}}^{0.86 \pm 0.04}$, with a slight reduction in σ_{int} from 0.39 ± 0.03 to 0.36 ± 0.03 . The best-fit $L_X - T_a - E_{\text{iso}}$ correlation and the constrains on the coefficients are displayed in Figure 1.

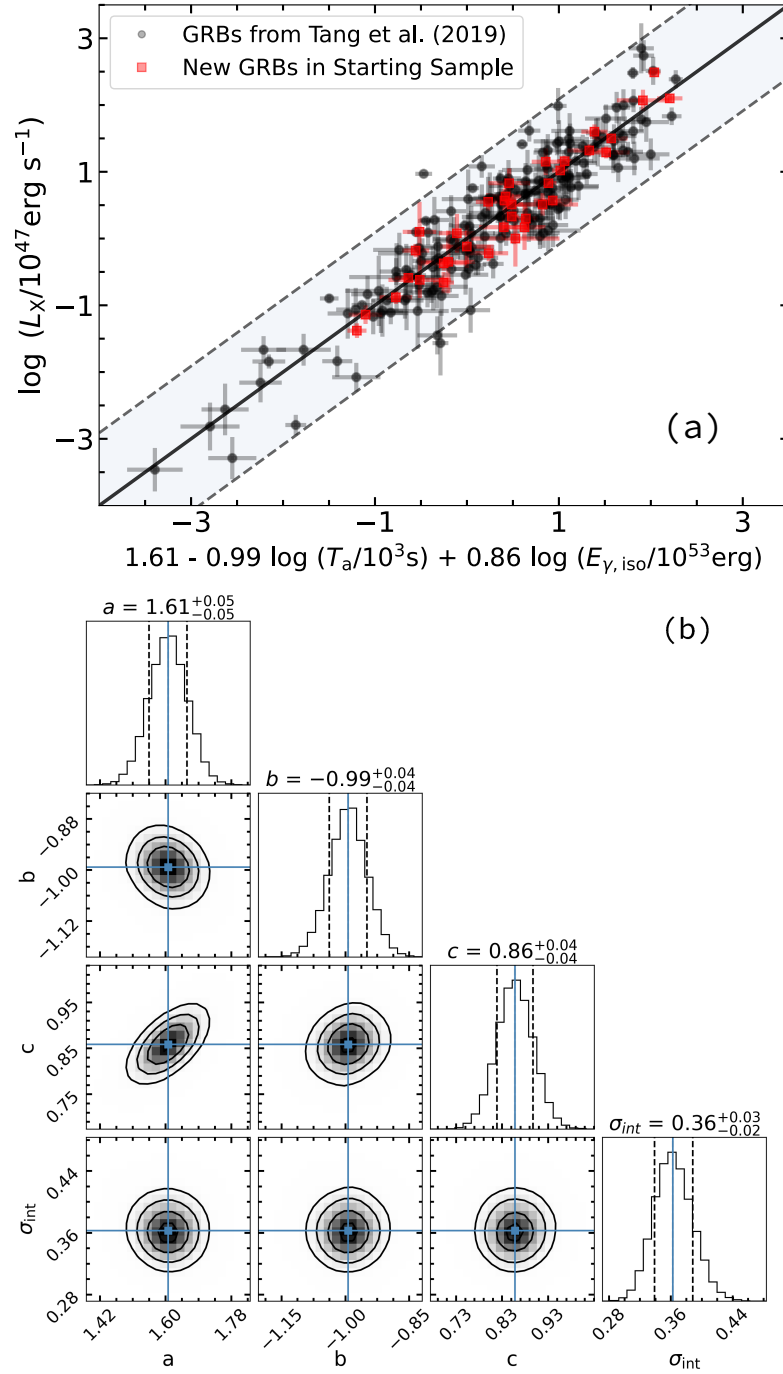


Figure 1. (a) The $L_X - T_a - E_{\text{iso}}$ correlation updated with 210 GRBs by Deng et al. [220]. The solid line and dashed lines denote the best-fit result and 3σ confidence level, respectively. The 174 GRBs from Tang et al. [219] are represented by black dots, and the red squares indicate the 36 new GRBs included in the analysis of Deng et al. [220]. (b) The posterior probability distributions of the fitting parameters in the $L_X - T_a - E_{\text{iso}}$ correlation from Deng et al. [220]. The vertical solid lines and dashed lines represent the mean values and 1σ confidence level, respectively.

From a physical perspective, the $L_X - T_a - E_{\text{iso}}$ correlation may indicate that the X-ray plateaus originate from central engine energy injection, akin to discussions surrounding the $L_X - T_a$ correlation. Xu et al. [218] proposed that the injected energy from the magnetar may manifest as relativistic positron-electron wind [221–223], a scenario similar to that employed by Geng et al. [212,224] to explain the late-time optical brightening observed in some GRBs. As the positron-electron wind interacts with the forward shock, it induces a

long-duration reverse shock that propagates through the wind itself, contributing to the shallow decay phase observed in the X-ray afterglow. A key advantage of this model is its explanation of the chromatic break observed in the afterglow phase, achieved by the combined contributions of multiple emission regions to the total flux. The X-ray plateau luminosity reflects the rate of energy injection from the central engine. Differences in the magnetic field strength and spin period of the nascent magnetar may account for the observed dispersion within this correlation. Dai et al. [221] demonstrated that the energy injected by the magnetar into the forward shock, which produces the observable plateau, should be comparable to the energy of the initial fireball that drives the prompt radiation. This is largely consistent with the $L_X - T_a - E_{\text{iso}}$ correlation, which essentially gives $L_X T_a \propto E_{\text{iso}}^{0.86}$.

2.2.3. The $E_{X,\text{iso}} - E_{\text{iso}} - E_p$ correlation

Bernardini et al. [225] discovered a tight three-parameter correlation in *Swift* GRBs involving the E_{iso} in the $1\text{-}10^4$ keV range, the peak energy E_p , and the isotropic equivalent energy $E_{X,\text{iso}}$ of X-ray afterglow in the 0.3-10 keV band. i.e.,

$$\log\left(\frac{E_{X,\text{iso}}}{\text{erg}}\right) = (1.06 \pm 0.06) \log\left(\frac{E_{\text{iso}}}{\text{erg}}\right) - (0.74 \pm 0.10) \log\left(\frac{E_p}{\text{keV}}\right) - (2.36 \pm 0.25). \quad (11)$$

The $E_{X,\text{iso}} - E_{\text{iso}} - E_p$ correlation was further examined in depth by Margutti et al. [226], wherein various observational correlations involving both prompt and afterglow parameters were also investigated. This correlation can be interpreted as arising from the inclusion of $E_{X,\text{iso}}$ as a third variable into the Amati relation, which reduces the intrinsic dispersion of the original relation. Notably, while SGRBs do not satisfy the Amati relation derived from LGRBs, both types of GRBs conform to the same $E_{X,\text{iso}} - E_{\text{iso}} - E_p$ correlation. This indicates long and short GRBs may share similar characteristics, offering insights into the underlying physics of both groups in a unified picture [226]. Subsequently, Zaninoni et al. [227] validated the $E_{X,\text{iso}} - E_{\text{iso}} - E_p$ correlation with an expanded sample. Although long and short GRBs adhere to the same $E_{X,\text{iso}} - E_{\text{iso}} - E_p$ correlation, they occupy separate regions in the 2D correlation plane. Furthermore, Zaninoni et al. [227] found that an intermediate group of GRBs exists between long and short GRBs in this 2D plane, which encompasses ultral-long GRBs and low-energy GRBs.

A two-parameter correlation involving E_p and ϵ serves as a convenient proxy for the $E_{X,\text{iso}} - E_{\text{iso}} - E_p$ correlation, where ϵ , defined as $\epsilon = E_{X,\text{iso}}/E_{\text{iso}}$, inversely represents the emission efficiency of GRBs. Bernardini et al. [225] found that $\epsilon \propto E_p^{-0.58}$. This finding suggests that the $E_{X,\text{iso}} - E_{\text{iso}} - E_p$ correlation may be connected with the Lorentz factor of the GRB jet, as a faster outflow converts more energy into the prompt phase. Additionally, the photospheric model provides a natural explanation for the $E_{X,\text{iso}} - E_{\text{iso}} - E_p$ correlation, since brighter GRBs exhibit a higher radiation efficiency [228]. The cannonball model has also been proposed as an alternative explanation for this correlation [229].

2.2.4. The Combo relation

Izzo et al. [230] analyzed a sample of 60 LGRBs. They combined the Amati relation with the $E_{X,\text{iso}} - E_{\text{iso}} - E_p$ correlation to derive a tight four-parameter correlation that involves both the prompt emission parameters and the afterglow parameters. It is called the Combo relation, which can be expressed as

$$\log\left(\frac{L_0}{\text{erg/s}}\right) = \log\left(\frac{A}{\text{erg/s}}\right) + \gamma\left(\log\left(\frac{E_p}{\text{keV}}\right) - \frac{1}{\gamma} \log\left(\frac{\tau/\text{s}}{|1 + \alpha_X|}\right)\right), \quad (12)$$

where L_0 , τ and α_X are the initial X-ray luminosity of the plateau phase, the end time of the plateau phase, and power-law decay index post the shallow phase, respectively. A phenomenological light curve expression, $L(t) = L_0(1 + t/\tau)^{\alpha_X}$ as proposed by Ruffini et al. [231], is adopted to fit the X-ray data and further derive the constant L_0 , which is

crucial for determining the Combo relation. The best fit parameters provided by Izzo et al. [230] are $\log[A/(\text{erg/s})] = 49.94 \pm 0.27$, $\gamma = 0.74 \pm 0.1$, and $\sigma_{\text{int}} = 0.33 \pm 0.04$. Muccino et al. [232] later confirmed the validity of this correlation with an expanded sample of 174 GRBs, updating the coefficients as $\log[A/(\text{erg/s})] = 49.66 \pm 0.2$, $\gamma = 0.84 \pm 0.08$, and $\sigma_{\text{int}} = 0.37 \pm 0.02$. The slope parameter γ remains largely constant across different redshift bins, indicating that the Combo relation does not evolve at different redshift.

Theoretically, the Combo relation reflects the connection between the prompt radiation and the X-ray afterglow, as well as the characteristics of GRB outflow and the surrounding environment [233]. Muccino et al. [233] used an external forward shock model, which accelerates electrons into a power-law distribution, to explain the physical origin of the Combo relation. In this framework, the parameters such as E_p , L_0 , and τ depend on the initial Lorentz factor of the GRB jet, and the different spectral energy distribution of the emitting source lead to the dispersion of the Combo relation.

3. Application of the Observed Correlations

3.1. Usage of the observed correlation in cosmology

An essential preliminary step in using GRBs to constrain cosmological model parameters is deriving the Hubble diagram of GRBs based on known empirical correlations. The Hubble diagram represents the relationship between redshift z and the distance modulus μ , defined as

$$\mu = 5 \log \frac{d_L}{\text{Mpc}} + 25 = 5 \log \frac{d_L}{\text{cm}} - 97.45. \quad (13)$$

Here d_L denotes the luminosity distance, which is expressed as

$$d_L = (1+z) \frac{C}{H_0} \begin{cases} \frac{1}{\sqrt{\Omega_k}} \sinh \left[\sqrt{\Omega_k} \int_0^z \frac{dz'}{\sqrt{E(z', \Omega_m, \Omega_\Lambda, w(z'))}} \right], & \Omega_k > 0, \\ \int_0^z \frac{dz'}{\sqrt{E(z', \Omega_m, \Omega_\Lambda, w(z'))}}, & \Omega_k = 0, \\ \frac{1}{\sqrt{|\Omega_k|}} \sin \left[\sqrt{|\Omega_k|} \int_0^z \frac{dz'}{\sqrt{E(z', \Omega_m, \Omega_\Lambda, w(z'))}} \right], & \Omega_k < 0, \end{cases} \quad (14)$$

where Ω_m , Ω_k , and Ω_Λ are the matter density parameter, space curvature, and dark energy density parameter, respectively. C and H_0 represent the speed of light and the Hubble constant, respectively. The specific form of $E(z, \Omega_m, \Omega_\Lambda, w(z))$ depends on the cosmological model and is generally defined as

$$E(z, \Omega_m, \Omega_\Lambda, w(z)) = \Omega_m(1+z)^3 + \Omega_k(1+z)^2 + \Omega_\Lambda e^3 \int_0^{\ln(1+z)} 1 + \omega(z') d \ln(1+z'), \quad (15)$$

where $\omega(z)$ denotes the equation of state (EOS) parameter of dark energy. In a parameterized CPL model [234,235], $\omega(z) = \omega_0 + \omega_a \frac{z}{1+z}$, representing the evolution of the dark energy EOS with redshift. When ω_a is set to 0 and ω_0 varies freely, we call it the ω CDM model. If ω_0 is further fixed at -1 , the model reduces to the standard Λ CDM model. Theoretically, one can identify the cosmological model and determine its parameters by fitting the observed GRB data.

3.1.1. Cosmology with the Amati relation

Amati et al. [151] utilized the Amati relation derived from a sample of 70 LGRBs and XRFs to constrain the Λ CDM cosmological parameters. Their results indicate that the matter density parameter Ω_m lies in a range of 0.05 – 0.40 for the flat assumption, and in 0.04 – 0.50 for the non-flat case, where the ranges correspond to the 1σ confidence level. Numerical simulations indicate that the uncertainty of cosmological parameters can be further reduced as the GRB sample size increases. Wang et al. [236] compiled

a sample of 151 LGRBs and calibrated the Amati relation using SNe Ia. The cosmology parameters derived by them are consistent with those derived based on SNe Ia observations, yielding $\Omega_m = 0.271 \pm 0.019$ for the flat Λ CDM universe, and $\Omega_m = 0.225 \pm 0.044$ and $\Omega_\Lambda = 0.640 \pm 0.082$ for the non-flat Λ CDM model. The precision of Ω_m was further enhanced by combining 221 LGRBs with the Pantheon SNe Ia sample [237], providing the best-fit parameters of $\Omega_m = 0.29 \pm 0.01$ for the flat Λ CDM model, and $\Omega_m = 0.34 \pm 0.04$ and $\Omega_\Lambda = 0.79 \pm 0.06$ for the non-flat Λ CDM scenario [238].

Due to the limited observational data for low-redshift GRBs (e.g., $z < 0.1$), establishing the empirical correlations depends on a pre-assumed cosmological model to derive isotropic equivalent energy or luminosity. When such a relation is directly applied for cosmology studies, the derived cosmological parameters become dependent on the prior cosmological model, known as the circularity problem [239]. A commonly employed method to address this circularity problem involves standardizing GRBs using SNe Ia data, as previously mentioned. However, the results derived from this approach should be interpreted with caution. This is because the systematics of SNe Ia could bias the GRB Hubble diagram, thereby amplifying the uncertainties associated with using GRBs as a cosmological probe. It is worth noting that Amati et al. [153] constrained Ω_m as ~ 0.3 by using GRB data alone, without requiring calibration with SNe Ia.

Moreover, the use of observational Hubble data (OHD) enables the calibration of the GRB luminosity correlation in a model-independent way [240–242]. The application of Bézier parametric curves [243,244] and Gaussian process methods [245–247] to fit the OHD is well-established in the literature. However, calibrating GRBs using external calibrators such as SNe Ia and OHD compromises their status as independent cosmological probes. In addition, the calibration process is typically performed at low redshift and subsequently extended to higher redshift regions. The reliability of such calibration methods depends on the assumption that the GRB luminosity correlations do not evolve with redshift. Redshift evolution may arise from selection biases and instrumental detection thresholds [118,153,248], making it crucial to assess its impact on the application of the luminosity correlation in cosmology. Taking the Amati relation as an example, although there is ongoing debate about the existence of redshift evolution, its impact on the robustness of the Amati relation across different redshifts is trivial [153,155,156,243]. Ghirlanda et al. [249] demonstrated that both the normalization factor and slope of the Amati relation are independent of redshift. Demianski et al. [155] divided a sample of 162 LGRBs into low- and high-redshift groups, with a redshift of 2 as the boundary. They showed that the constrained results of the Λ CDM and CPL models for the two groups were consistent within 1σ error.

Other promising approaches to address the circularity problem involve performing self-calibration within a narrow redshift bin, or simultaneously fitting the parameters for the luminosity correlation and cosmological models, without relying on a background cosmological model. The quality of GRB samples is critical for establishing GRBs as reliable independent cosmological probes. Khadka et al. [250] performed a comprehensive analysis of six cosmological models using the Amati relation, applied to a meticulously compiled sample of 119 GRBs through the simultaneous fitting method. Their findings confirmed that the parameters of the Amati relation are model-independent, underscoring its effectiveness in standardizing GRBs as reliable cosmological probes. This represented the first demonstration of such a result for GRBs. After excluding one GRB with insecure redshift measurement, the remaining 118 GRBs, i.e., A118 dataset [250–255], exhibited low intrinsic dispersion and formed a consistent Amati relation GRB sample [251]. Additionally, Cao et al. [255–257] conducted robust joint constraint analyses on various cosmological models by integrating GRBs standardized with the Amati relation alongside other well-established cosmological probes. Their study validated the consistency among different observational datasets and provided evidence supporting the dark energy dynamics and the existence of spatial curvature [255–257].

3.1.2. Cosmology with the Yonetoku relation

Kodama et al. [239] calibrated the Yonetoku relation in a model-independent way with 33 LGRBs with known redshifts below 1.62. With additional 30 GRBs with redshifts ranging from 1.8 to 5.6, they applied the calibrated Yonetoku relation on a flat universe to get $\Omega_m = 0.37^{+0.14}_{-0.11}$ at the 1σ confidence level. For the non-flat Λ CDM model, the most likely parameters are derived as $\Omega_m = 0.25^{+0.27}_{-0.14}$ and $\Omega_\Lambda = 1.25^{+0.10}_{-1.25}$. Using a similar calibration method, Tsutsui et al. [258] compared the cosmology parameters derived by using the Yonetoku relation and the Amati relation. They found that the results of the two methods are consistent at the 2σ level, but are obviously different at the 1σ level. Additionally, the Hubble diagrams derived from these two relations exhibit a systematic difference in the high-redshift region. In another study, Tsutsui et al. [259] also used 63 GRBs and 192 SNe to investigate the flat ω CDM and CPL models. They found that the resultant cosmology parameters are consistent with the standard Λ CDM model at the 2σ level.

3.1.3. Cosmology with the Dainotti relation

The usage of the Dainotti relation as an independent cosmology probe was first proposed by Cardone et al [194]. They gathered a sample of 66 GRBs with a plateau phase in their X-ray afterglow and constructed the Hubble diagram with the data set. The standard Λ CDM model, ω CDM model and CPL model were tested by them. For the Λ CDM model and ω CDM model, the results derived by using the Dainotti relation are consistent with previous studies, indicating that the GRB data does not introduce systematic biases on the cosmology parameters and affirming the effectiveness of the afterglow relation in cosmology researches. For the CPL model, the cosmology parameters are not well constrained, but are still in broad consistency with the standard Λ CDM model at the 1σ confidence level. Using a sample of 68 LGRBs, Postnikov et al. [199] applied the Dainotti relation to study the evolution of the dark energy EOS parameter ω with redshift. They adopted a non-parametric method. The observational data of SNe Ia and baryonic acoustic oscillations (BAOs) are also incorporated. The ω parameter derived by them is close to the constant of -1 , consistent with the standard Λ CDM model.

Wang et al. [246] analyzed 31 LGRBs with a plateau phase in the X-ray light curve. For all these events, the post-plateau decay follows a temporal power-law index of -2 . Such a decaying pattern can be well described by the energy injection process due to the spin-down of a magnetar. Since the same energy injection mechanism is likely involved in all these GRBs, they argued that these GRBs could serve as more reliable standard candles. After standardizing the sample using the Dainotti relation, they applied these GRBs to study various cosmology models. The Hubble diagram derived by them are generally consistent with previous results across both low and high redshifts. Interestingly, a 3σ -level evidence for cosmic acceleration was revealed. Hu et al. [247] utilized the OHD to alleviate the circularity problem and constrained the cosmology parameters by combining 31 LGRBs from Wang et al. [246]. 5 additional SGRBs, whose X-ray afterglow is dominated by magnetic dipole radiation, are also included. For the non-flat Λ CDM model, the best-fit parameters are $\Omega_m = 0.33^{+0.06}_{-0.09}$ and $\Omega_\Lambda = 1.06^{+0.15}_{-0.34}$ at the 1σ level. Further considering the Pantheon SNe Ia sample, they obtained $\omega = -1.11^{+0.11}_{-0.15}$ and $\Omega_m = 0.34^{+0.05}_{-0.04}$ for the flat ω CDM universe. They concluded that the standard Λ CDM model still remains to be the preferred model. Additionally, the Dainotti relation drawn from optical and radio samples has also been used to investigate the universe [260,261], which gives consistent results with that using X-ray afterglows.

Cao et al. [262] utilized three datasets from Wang et al. [246] and Hu et al. [247] to apply the 2D Dainotti relation to constrain the six cosmological models. Despite the relatively weak constraints derived from the 2D Dainotti relation, they remain consistent with those obtained from the OHD + BAO data, yielding $\Omega_m \sim 0.3$, thus demonstrating the potential of the Dainotti relation for standardizing GRBs. Using the platinum sample defined by Dainotti et al. [204,205], Cao et al. [263] confirmed the reliability of the 3D Dainotti relation

in standardizing GRBs. The combination of the 3D Dainotti relation and the Amati relation yields better constraints compared to the 3D Dainotti relation alone. However, the precision remains inferior to that achieved by the OHD + BAO data, indicating that current GRB data alone are insufficient for providing strict cosmological constraints [263]. Moreover, a detailed comparative analysis indicated that the 3D Dainotti relation outperforms the 2D Dainotti in standardizing GRBs, exhibiting improved parameter consistency across various cosmological models [264].

3.1.4. Cosmology with the $L_X - T_a - E_p$ correlation

Xu et al. [265] argued that the $L_X - T_a - E_{\text{iso}}$ correlation is redshift-dependent. Furthermore, since both L_X and E_{iso} depends on the redshift in a similar form, this correlation is insensitive to cosmology parameters and thus is unsuitable for cosmology study. They then combined the Amati relation and the $L_X - T_a - E_{\text{iso}}$ correlation to derive a new three-parameter correlation as $L_X \propto T_a^{-1.08 \pm 0.8} E_p^{0.76 \pm 0.14}$, with an intrinsic scatter of $\sigma_{\text{int}} = 0.54 \pm 0.04$. This expression is named as the $L_X - T_a - E_p$ correlation, which is also affected by redshift evolution. Xu et al. [265] used the EP method to mitigate this effect. The $L_X - T_a - E_p$ correlation is somewhat analogous to the Combo relation. Although the $L_X - T_a - E_p$ correlation itself is insufficient to constrain cosmology parameters satisfactorily, Xu et al. [265] argued that it can be combined with the cosmic microwave background (CMB), SNe Ia, and BAO data to constrain the parameters of various cosmological models, as shown in Figure 2. They derived $\Omega_m = 0.291 \pm 0.005$ for the flat Λ CDM model, $\Omega_m = 0.289 \pm 0.008$ and $\Omega_\Lambda = 0.710 \pm 0.006$ for the non-flat Λ CDM model, and $\Omega_m = 0.295 \pm 0.006$ and $\omega = -1.015 \pm 0.015$ for the flat ω CDM model.

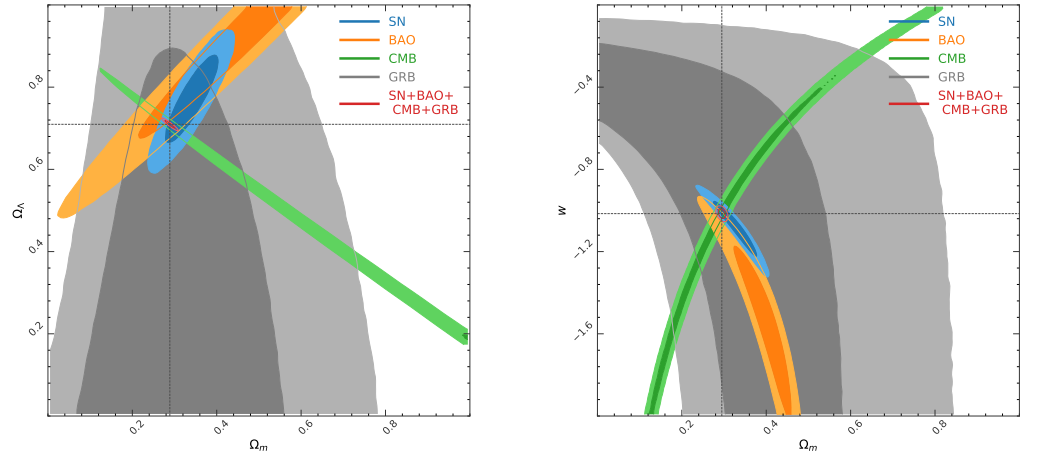


Figure 2. The joint constraints for the non-flat Λ CDM model (left-hand panel) and flat ω CDM model (right-hand panel) by Xu et al. [265]. The observational data of SNe Ia, BAO, CMB, and the $L_X - T_a - E_p$ correlation of GRBs are depicted in blue, orange, green, and gray, respectively. The dashed lines indicate the best-fit values for the two models: $\Omega_m = 0.289 \pm 0.008$ and $\Omega_\Lambda = 0.710 \pm 0.006$ for the non-flat Λ CDM model, and $\Omega_m = 0.295 \pm 0.006$ and $\omega = -1.015 \pm 0.015$ for the flat ω CDM model.

Interestingly, for optical afterglows with a plateau phase, there also exists a three parameter correlation similar to the $L_X - T_a - E_p$ relation. The optical afterglow sample have also been utilized to investigate the $X_1 X_2$ CDM model, in which the dark energy is comprised of two independent components [261]. According to the Bayesian information criterion, the ω CDM model with a single dark energy component is preferred over the $X_1 X_2$ CDM model.

3.1.5. Cosmology with the Combo relation

Izzo et al. [230] employed the Combo relation to constrain the parameters of various cosmology models, using a calibration technique designed to minimize the dependence on SNe Ia. Adopting 60 LGRBs alone, they obtained the best-fit parameters as $\Omega_m = 0.29_{-0.15}^{+0.23}$ for the flat Λ CDM model, and $\Omega_m = 0.40_{-0.16}^{+0.22}$, $\omega = -1.43_{-0.66}^{+0.78}$ for the flat ω CDM model. Here the error ranges are all corresponding to the 1σ level. Note that their results for the CPL model align with the standard Λ CDM universe, although the uncertainties of the derived parameters are still relatively large. Muccino et al. [232] expanded the sample size to 174 LGRBs. They utilized the Combo relation to obtain a much tighter constraints on the cosmological parameters. When using $H_0 = (74.03 \pm 0.5) \text{ km s}^{-1} \text{ Mpc}^{-1}$ [266] as a prior for the Hubble constant, the updated parameters are $\Omega_m = 0.32_{-0.05}^{+0.05}$ for a flat Λ CDM universe, and $\Omega_m = 0.34_{-0.07}^{+0.08}$, $\Omega_\Lambda = 0.91_{-0.35}^{+0.22}$ for a non-flat Λ CDM model. On the other hand, when they use $H_0 = (67.4 \pm 1.42) \text{ km s}^{-1} \text{ Mpc}^{-1}$ [267] as the prior, the derived parameters are $\Omega_m = 0.22_{-0.03}^{+0.04}$ for the flat Λ CDM universe, while $\Omega_m = 0.24_{-0.05}^{+0.06}$, $\Omega_\Lambda = 1.01_{-0.25}^{+0.15}$ for the non-flat Λ CDM universe. Moreover, Muccino et al. [232] demonstrated that the $\omega(z)$ parameter is consistent with the Λ CDM model in the low-redshift region. However, at high redshifts, $\omega(z)$ deviates from the standard value of -1 .

Khadka et al. [251] conducted a comprehensive analysis of five datasets. They used the Combo relation to constrain the six cosmological models, employing the simultaneous fitting technique to bypass the circularity problem. The results revealed moderate inconsistencies in the parameters of the Combo relation across various cosmological models, leading to the conclusion that the five Combo relation datasets analyzed in the study are unreliable for constraining cosmological parameters. Furthermore, the intrinsic dispersion parameter of the dataset is found unsuitable to act as a metric for evaluating the robustness of cosmological constraints [251].

3.2. Pseudo-redshifts calculated by using the correlations

After over 20 years of observations, redshift information has been obtained for a substantial number of GRBs, allowing us to infer their luminosity distances and to utilize them for cosmological researches. However, for many GRBs, the redshifts are still unavailable. The most distant GRB has a redshift of approximately 9.4 [115], yet some GRBs without redshift measurements may originate from even earlier cosmic epochs. Empirical correlations observed in the prompt and afterglow phases may offer insights on the redshifts of these GRBs. However, most of these correlations exhibit considerable dispersion, leading to significant uncertainty in the derived redshift. So, the redshifts calculated by using these empirical correlations are called pseudo-redshifts. In this subsection, we briefly summarize various efforts trying to calculate pseudo-redshifts from GRB correlations.

3.2.1. A redshift indicator related to the Amati relation

Based on the Amati relation, Atteia [268] found that a combination of some observed quantities in GRB prompt phase shows a weak dependence on the isotropic equivalent energy, suggesting its potential as a redshift indicator. The combined parameter, denoted as X , is defined as $X = n_\gamma / (E_p T_{90}^{0.5})$, where n_γ represents the observed photon numbers between $E_p/100$ and $E_p/2$. X depends on the redshift as

$$X = A \times f(z), \quad (16)$$

where A is a normalization parameter and $f(z)$ refers to the redshift evolution of X derived from a ‘‘standard’’ GRB in a standard Λ CDM universe. The energy spectrum of prompt GRB emission can be described by the so called Band function, with typical power-law indices of $\alpha = -1.0$, $\beta = -2.3$, and characteristic energy of $E_p = 250 \text{ keV}$. The pseudo-redshift, z_{est} , can then be calculated as $z_{\text{est}} = f^{-1}(X)/A$. The pseudo-redshift calculated in this way may have an uncertainty up to a factor two, but it allows one to quickly identify high-redshift GRBs.

3.2.2. Pseudo-redshifts from the Yonetoku relation

The pseudo-redshift of a GRB can also be derived by inversely applying the best-fitting Yonetoku relation. For this purpose, Yonetoku et al. [173] set a flux threshold to ensure a higher signal-to-noise ratio, excluding those weak GRBs whose pseudo-redshift could not be credibly determined. A sample of 689 BATSE GRBs, with time-averaged energy spectra in the prompt phase described by the Band function [74] were collected. The pseudo-redshifts were calculated for them, and were further used to investigate the evolution of the GRB formation rate over redshift.

Additionally, Tsutsui et al. [180] derived the best-fit Yonetoku relation from 8 well-defined SGRBs. Their results can be expressed as

$$\frac{d_L^2}{(1+z)^{1.59}} = \frac{10^{52.29} \text{ erg s}^{-1}}{4\pi F_p} \left(\frac{E_{p,\text{obs}}}{774.5 \text{ keV}} \right)^{1.59}, \quad (17)$$

where F_p , and $E_{p,\text{obs}}$ are the peak flux and peak energy of the prompt energy spectrum in the observer's frame, respectively. The right hand side of Equation (17) involves observational quantities in the prompt phase, while the left hand side is a function of redshift. Using this equation, the pseudo-redshifts can be easily determined. They applied the method to a sample of 71 bright BATSE SGRBs and found that their pseudo-redshifts range from 0.097 to 2.258, with a mean of 1.05.

3.2.3. Pseudo-redshift from the Dainotti relation

Dainotti et al. [269] explored the potential of using the Dainotti relation, involving only afterglow parameters, to calculate the pseudo-redshift. For this purpose, the best-fit Dainotti relation was re-organized and expressed as

$$\begin{aligned} \log L_X &= \log(4\pi F_X) + 2 \log d_L - (1 - \beta_a) \log(1+z) \\ &= a \log\left(\frac{T_a}{1+z}\right) + b, \end{aligned} \quad (18)$$

where a and b are the coefficient parameters in the Dainotti relation, β_a denotes the spectral index of the X-ray afterglow, and F_X is the X-ray flux at the end of the plateau phase. By solving the above nonlinear function for a particular GRB, the pseudo-redshifts can be obtained. However, Dainotti et al. [269] demonstrated that the pseudo-redshifts derived from Equation (18) are somewhat uncertain due to significant influences from the errors in the observed quantities, the precision of fitting parameters a and b , and the intrinsic dispersion σ_{int} , which contributes nonlinearly to the overall error. These issues may be alleviated with a larger, high-quality GRB sample. Moreover, the 3D Dainotti relation [204,205], combined with the platinum sample selected through strict criteria, may help give a much better estimate of the redshift due to its significantly smaller intrinsic dispersion as compared to the 2D Dainotti relation.

3.2.4. Pseudo-redshifts from the $L_X - T_a - E_{\text{iso}}$ correlation

Deng et al. [220] argued that the three parameter $L_X - T_a - E_{\text{iso}}$ correlation can also be used to calculate the pseudo-redshift. They collected a sample of 210 GRBs with a plateau phase in the X-ray afterglow, all with known redshift. They referred the sample as the Starting Sample, from which a best-fit $L_X - T_a - E_{\text{iso}}$ correlation is updated by using

the MCMC method. A redshift correlation function, $g(z)$, is then derived based on the $L_X - T_a - E_{\text{iso}}$ correlation as

$$\begin{aligned}
 g(z) &= \log\left(\frac{L_X}{10^{47} \text{ erg s}^{-1}}\right) - a - b \log\left(\frac{T_a}{10^3 \text{ s}}\right) - c \log\left(\frac{E_{\text{iso}}}{10^{53} \text{ erg}}\right) \\
 &= (2 - 2c) \log\left(\int_0^z \frac{1}{\sqrt{(1+z')^3 \Omega_m + \Omega_\Lambda}} dz'\right) + (b + c + \beta_X - c\alpha_\gamma) \log(1+z) \\
 &\quad - c \log(4\pi S) + \log(4\pi F_X) - a - b \log(T_{a,\text{obs}}) \\
 &\quad + 3b - 47 + 53c + (2 - 2c) \log\left(\frac{C}{H_0}\right),
 \end{aligned} \tag{19}$$

where $T_{a,\text{obs}}$ is the end time of the plateau in the observer's frame, and a , b , and c are coefficient parameters in the $L_X - T_a - E_{\text{iso}}$ correlation. S and α_γ represent the fluence in 15 – 150 keV and the photon spectral index as observed by *Swift* BAT, respectively. Deng et al. [220] then collected another sample of 130 GRBs with a plateau phase but without redshift measurement, which is called the Target Sample. They tried to calculate the pseudo-redshifts of these Target Sample GRBs by using the $L_X - T_a - E_{\text{iso}}$ correlation. Substituting the observed F_X , S , $T_{a,\text{obs}}$ and α_γ values of the Target sample into Equation (19), the redshifts can be conveniently derived. In the process, it was found that a reasonable solution could not be obtained for 22 GRBs, which means the pseudo-redshift is unavailable in context of the $L_X - T_a - E_{\text{iso}}$ correlation. Ultimately, the pseudo-redshifts are calculated for 108 GRBs by using this method. Deng et al. [220] went further to utilize both the Starting Sample and the Target Sample to check the Dainotti relation and the $\bar{L}_{\gamma,90} - L_X$ correlation, where $\bar{L}_{\gamma,90} = E_{\text{iso}}/T_{90}$ represents the average luminosity in the prompt phase. The best-fit Dainotti relations obtained from the samples are consistent with each other within 1σ error. However, although a tight $\bar{L}_{\gamma,90} - L_X$ correlation is observed in the Target Sample, its slope differs significantly from that of the Starting Sample. The cause of this difference is still unknown and warrants further investigation in the future.

4. Conclusions

In this review, several empirical correlations in GRBs, covering various observed parameters involving both prompt and afterglow phases, are introduced. The correlations reveal key relationships among GRB parameters, providing constraints on the radiation mechanisms and insights into the composition and structure of GRB jets. Possible physical interpretations of these correlations are discussed. Their applications in cosmology researches are also highlighted. Finally, various approaches of calculating the pseudo-redshifts of GRBs based on the observed correlations are briefly outlined.

It is interesting to note that for some empirical correlations, the detailed expressions are different for long GRBs and short GRBs, indicating inherent population differences possibly related to their central engines or progenitors. On the other hand, for several other correlations, both long GRBs and short GRBs have the same function form, highlighting their shared features. Despite these insights, it remains challenging to use empirical correlations as definitive model discriminators due to the uncertain physical interpretations of these relationships. Therefore, further theoretical investigations, including detailed studies of GRB dynamics, radiation processes are essential. Numerical simulations of the jet dynamics and the particle acceleration will also be helpful. Additionally, the afterglow data could provide important constraints on the GRB radiation efficiency and jet structure. Note that many afterglow correlations pertain to the plateau phase, which strongly indicates the plateau phase may have a unique origin. Precise multi-wavelength afterglow observations beyond the X-ray data could yield new insights. For example, breaks in the afterglow light curves, either achromatic or chromatic, could provide key information on the beaming effects and/or the radiation mechanisms.

GRBs could potentially help probe the universe at high-redshift, enabling access to earlier cosmic epochs than SNe Ia. However, employing GRBs as standard candles

requires reliable empirical correlations, whose robustness depends closely on the physical classification of GRBs. Additionally, some physical parameters involved in the correlations may evolve with redshift or be affected by selection effects related to detector sensitivity [248]. Therefore, effective calibrations are critical to correct for such effects and to effectively constrain cosmological parameters.

A widely used method for standardizing GRBs involves calibrating them with SNe Ia data at low redshifts [155,239,258,265], partially mitigating the circularity problem. However, the joint analysis of SNe Ia and GRBs assigns significant statistical weights to SNe Ia, leading to results dominated by SNe Ia and compromising the independence of GRBs as a cosmological probe. Currently, some empirical correlations, such as the Amati and Dainotti relations, are recognized as cosmology-independent and serve as reliable tools for standardizing GRBs [250,251,262–264]. Nonetheless, even high-quality datasets, such as A118 sample [250–255], yield relatively weak cosmological constraints. They are consistent with the constraints from OHD + BAO data but fail to substantially enhance the precision. While GRB data provide valuable complementary constraints to other well-established cosmological probes, improving the precision requires higher-quality data. Striking a balance between intrinsic dispersion and sample size is essential [264].

Employing empirical correlations as redshift indicators for GRBs presents an intriguing approach. Nevertheless, limitations in sample quality, sample size, and intrinsic scatter of the correlations make them more suitable for statistical analysis of large samples rather than for reliably estimating the redshift of individual GRBs. Rigorous sample selection and exploration of novel fitting methods could enhance the reliability of empirical correlations for this purpose. Furthermore, machine learning approaches for GRB redshift estimation offer a promising direction for future researches [270–273].

The recently launched Chinese-French satellite, Space-based multiband astronomical Variable Objects Monitor (SVOM) [274], and the Einstein Probe [275], along with the upcoming Transient High-Energy Sky and Early Universe Surveyor (THESEUS) space missions [276], will discover more GRBs and will help us build high-quality GRB samples. The robustness of currently known empirical correlations is expected to be enhanced, and more new correlations may even be revealed, which would facilitate more precise investigation of the cosmic evolution history at high redshifts [117], address the Hubble tension [277], and refine GRB classification [66].

Acknowledgments: The authors are grateful to the anonymous referees for helpful suggestions. C. D. thanks J. P. Hu for valuable discussions. This study was supported by the National Key R&D Program of China (2021YFA0718500), the National Natural Science Foundation of China (Grant Nos. 12233002 and 12041306), the National SKA Program of China No. 2020SKA0120300, and the Natural Science Foundation of Xinjiang Uygur Autonomous Region (No. 2022D01A363). YFH also acknowledges the support from the Xinjiang Tianchi Program. AK also acknowledges the support from the Tianchi Talents Project of Xinjiang Uygur Autonomous Region.

Conflicts of Interest: The authors declare no conflicts of interest.

References

1. Kumar, P.; Zhang, B. The physics of gamma-ray bursts & relativistic jets. *Physics Reports* **2015**, *561*, 1–109, [arXiv:astro-ph.HE/1410.0679]. <https://doi.org/10.1016/j.physrep.2014.09.008>.
2. Gehrels, N.; Razzaque, S. Gamma-ray bursts in the swift-Fermi era. *Frontiers of Physics* **2013**, *8*, 661–678, [arXiv:astro-ph.HE/1301.0840]. <https://doi.org/10.1007/s11467-013-0282-3>.
3. Nakar, E. Short-hard gamma-ray bursts. *Physics Reports* **2007**, *442*, 166–236, [arXiv:astro-ph/0701748]. <https://doi.org/10.1016/j.physrep.2007.02.005>.
4. Zhang, B. *The Physics of Gamma-Ray Bursts*; 2018. <https://doi.org/10.1017/9781139226530>.
5. Berger, E. Short-Duration Gamma-Ray Bursts. *Annual Review of Astronomy and Astrophysics* **2014**, *52*, 43–105, [arXiv:astro-ph.HE/1311.2603]. <https://doi.org/10.1146/annurev-astro-081913-035926>.
6. Piran, T. The physics of gamma-ray bursts. *Reviews of Modern Physics* **2004**, *76*, 1143–1210, [arXiv:astro-ph/0405503]. <https://doi.org/10.1103/RevModPhys.76.1143>.
7. Boella, G.; Butler, R.C.; Perola, G.C.; Piro, L.; Scarsi, L.; Bleeker, J.A.M. BeppoSAX, the wide band mission for X-ray astronomy. *Astronomy and Astrophysics Supplement Series* **1997**, *122*, 299–307. <https://doi.org/10.1051/aas:1997136>.

8. Fishman, G.J.; Meegan, C.A.; Wilson, R.B.; Brock, M.N.; Horack, J.M.; Kouveliotou, C.; Howard, S.; Paciesas, W.S.; Briggs, M.S.; Pendleton, G.N.; et al. The First BATSE Gamma-Ray Burst Catalog. *The Astrophysical Journal Supplement Series* **1994**, *92*, 229. <https://doi.org/10.1086/191968>.
9. Aptekar, R.L.; Frederiks, D.D.; Golenetskii, S.V.; Ilynskii, V.N.; Mazets, E.P.; Panov, V.N.; Sokolova, Z.J.; Terekhov, M.M.; Sheshin, L.O.; Cline, T.L.; et al. Konus-W Gamma-Ray Burst Experiment for the GGS Wind Spacecraft. *Space Science Reviews* **1995**, *71*, 265–272. <https://doi.org/10.1007/BF00751332>.
10. Ubertini, P.; Lebrun, F.; Di Cocco, G.; Bazzano, A.; Bird, A.J.; Broenstad, K.; Goldwurm, A.; La Rosa, G.; Labanti, C.; Laurent, P.; et al. IBIS: The Imager on-board INTEGRAL. *Astronomy and Astrophysics* **2003**, *411*, L131–L139. <https://doi.org/10.1051/0004-6361:20031224>.
11. Gehrels, N.; Chincarini, G.; Giommi, P.; Mason, K.O.; Nousek, J.A.; Wells, A.A.; White, N.E.; Barthelmy, S.D.; Burrows, D.N.; Cominsky, L.R.; et al. The Swift Gamma-Ray Burst Mission. *The Astrophysical Journal* **2004**, *611*, 1005–1020, [[arXiv:astro-ph/0405233](https://arxiv.org/abs/astro-ph/0405233)]. <https://doi.org/10.1086/422091>.
12. Barthelmy, S.D.; Barbier, L.M.; Cummings, J.R.; Fenimore, E.E.; Gehrels, N.; Hullinger, D.; Krimm, H.A.; Markwardt, C.B.; Palmer, D.M.; Parsons, A.; et al. The Burst Alert Telescope (BAT) on the SWIFT Midex Mission. *Space Science Reviews* **2005**, *120*, 143–164, [[arXiv:astro-ph/0507410](https://arxiv.org/abs/astro-ph/0507410)]. <https://doi.org/10.1007/s11214-005-5096-3>.
13. Meegan, C.; Lichti, G.; Bhat, P.N.; Bissaldi, E.; Briggs, M.S.; Connaughton, V.; Diehl, R.; Fishman, G.; Greiner, J.; Hoover, A.S.; et al. The Fermi Gamma-ray Burst Monitor. *The Astrophysical Journal* **2009**, *702*, 791–804, [[arXiv:astro-ph.IM/0908.0450](https://arxiv.org/abs/astro-ph.IM/0908.0450)]. <https://doi.org/10.1088/0004-637X/702/1/791>.
14. Briggs, M.S.; Paciesas, W.S.; Pendleton, G.N.; Meegan, C.A.; Fishman, G.J.; Horack, J.M.; Brock, M.N.; Kouveliotou, C.; Hartmann, D.H.; Hakkila, J. BATSE Observations of the Large-Scale Isotropy of Gamma-Ray Bursts. *The Astrophysical Journal* **1996**, *459*, 40, [[arXiv:astro-ph/9509078](https://arxiv.org/abs/astro-ph/9509078)]. <https://doi.org/10.1086/176867>.
15. Balazs, L.G.; Meszaros, A.; Horvath, I. Anisotropy of the sky distribution of gamma-ray bursts. *Astronomy and Astrophysics* **1998**, *339*, 1–6, [[arXiv:astro-ph/9807006](https://arxiv.org/abs/astro-ph/9807006)]. <https://doi.org/10.48550/arXiv.astro-ph/9807006>.
16. Tarnopolski, M. Testing the anisotropy in the angular distribution of Fermi/GBM gamma-ray bursts. *Monthly Notices of the Royal Astronomical Society* **2017**, *472*, 4819–4831, [[arXiv:astro-ph.HE/1512.02865](https://arxiv.org/abs/astro-ph.HE/1512.02865)]. <https://doi.org/10.1093/mnras/stx2356>.
17. Vavrek, R.; Balázs, L.G.; Mészáros, A.; Horváth, I.; Bagoly, Z. Testing the randomness in the sky-distribution of gamma-ray bursts. *Monthly Notices of the Royal Astronomical Society* **2008**, *391*, 1741–1748, [[arXiv:astro-ph/0806.3932](https://arxiv.org/abs/astro-ph/0806.3932)]. <https://doi.org/10.1111/j.1365-2966.2008.13635.x>.
18. Mészáros, A.; Bagoly, Z.; Horváth, I.; Balázs, L.G.; Vavrek, R. A Remarkable Angular Distribution of the Intermediate Subclass of Gamma-Ray Bursts. *The Astrophysical Journal* **2000**, *539*, 98–101, [[arXiv:astro-ph/0003284](https://arxiv.org/abs/astro-ph/0003284)]. <https://doi.org/10.1086/309193>.
19. Metzger, M.R.; Djorgovski, S.G.; Kulkarni, S.R.; Steidel, C.C.; Adelberger, K.L.; Frail, D.A.; Costa, E.; Frontera, F. Spectral constraints on the redshift of the optical counterpart to the γ -ray burst of 8 May 1997. *Nature* **1997**, *387*, 878–880. <https://doi.org/10.1038/43132>.
20. Kouveliotou, C.; Meegan, C.A.; Fishman, G.J.; Bhat, N.P.; Briggs, M.S.; Koshut, T.M.; Paciesas, W.S.; Pendleton, G.N. Identification of Two Classes of Gamma-Ray Bursts. *The Astrophysical Journal* **1993**, *413*, L101. <https://doi.org/10.1086/186969>.
21. Hjorth, J.; Sollerman, J.; Møller, P.; Fynbo, J.P.U.; Woosley, S.E.; Kouveliotou, C.; Tanvir, N.R.; Greiner, J.; Andersen, M.I.; Castro-Tirado, A.J.; et al. A very energetic supernova associated with the γ -ray burst of 29 March 2003. *Nature* **2003**, *423*, 847–850, [[arXiv:astro-ph/0306347](https://arxiv.org/abs/astro-ph/0306347)]. <https://doi.org/10.1038/nature01750>.
22. Malesani, D.; Tagliaferri, G.; Chincarini, G.; Covino, S.; Della Valle, M.; Fugazza, D.; Mazzali, P.A.; Zerbi, F.M.; D’Avanzo, P.; Kalogerakos, S.; et al. SN 2003lw and GRB 031203: A Bright Supernova for a Faint Gamma-Ray Burst. *The Astrophysical Journal* **2004**, *609*, L5–L8, [[arXiv:astro-ph/0405449](https://arxiv.org/abs/astro-ph/0405449)]. <https://doi.org/10.1086/422684>.
23. Woosley, S.E.; Bloom, J.S. The Supernova Gamma-Ray Burst Connection. *Annual Review of Astronomy and Astrophysics* **2006**, *44*, 507–556, [[arXiv:astro-ph/0609142](https://arxiv.org/abs/astro-ph/0609142)]. <https://doi.org/10.1146/annurev.astro.43.072103.150558>.
24. Sparre, M.; Sollerman, J.; Fynbo, J.P.U.; Malesani, D.; Goldoni, P.; de Ugarte Postigo, A.; Covino, S.; D’Elia, V.; Flores, H.; Hammer, F.; et al. Spectroscopic Evidence for SN 2010ma Associated with GRB 101219B. *The Astrophysical Journal* **2011**, *735*, L24, [[arXiv:astro-ph.CO/1105.0422](https://arxiv.org/abs/astro-ph.CO/1105.0422)]. <https://doi.org/10.1088/2041-8205/735/1/L24>.
25. Schulze, S.; Malesani, D.; Cucchiara, A.; Tanvir, N.R.; Krühler, T.; de Ugarte Postigo, A.; Leloudas, G.; Lyman, J.; Bersier, D.; Wiersema, K.; et al. GRB 120422A/SN 2012bz: Bridging the gap between low- and high-luminosity gamma-ray bursts. *Astronomy and Astrophysics* **2014**, *566*, A102, [[arXiv:astro-ph.HE/1401.3774](https://arxiv.org/abs/astro-ph.HE/1401.3774)]. <https://doi.org/10.1051/0004-6361/201423387>.
26. Campana, S.; Mangano, V.; Blustin, A.J.; Brown, P.; Burrows, D.N.; Chincarini, G.; Cummings, J.R.; Cusumano, G.; Della Valle, M.; Malesani, D.; et al. The association of GRB 060218 with a supernova and the evolution of the shock wave. *Nature* **2006**, *442*, 1008–1010, [[arXiv:astro-ph/0603279](https://arxiv.org/abs/astro-ph/0603279)]. <https://doi.org/10.1038/nature04892>.
27. Bloom, J.S.; Kulkarni, S.R.; Djorgovski, S.G.; Eichelberger, A.C.; Côté, P.; Blakeslee, J.P.; Odewahn, S.C.; Harrison, F.A.; Frail, D.A.; Filippenko, A.V.; et al. The unusual afterglow of the γ -ray burst of 26 March 1998 as evidence for a supernova connection. *Nature* **1999**, *401*, 453–456, [[arXiv:astro-ph/9905301](https://arxiv.org/abs/astro-ph/9905301)]. <https://doi.org/10.1038/46744>.
28. Galama, T.J.; Vreeswijk, P.M.; van Paradijs, J.; Kouveliotou, C.; Augusteijn, T.; Bönhardt, H.; Brewer, J.P.; Doublier, V.; Gonzalez, J.F.; Leibundgut, B.; et al. An unusual supernova in the error box of the γ -ray burst of 25 April 1998. *Nature* **1998**, *395*, 670–672, [[arXiv:astro-ph/9806175](https://arxiv.org/abs/astro-ph/9806175)]. <https://doi.org/10.1038/27150>.

29. Fruchter, A.S.; Levan, A.J.; Strolger, L.; Vreeswijk, P.M.; Thorsett, S.E.; Bersier, D.; Burud, I.; Castro Cerón, J.M.; Castro-Tirado, A.J.; Conselice, C.; et al. Long γ -ray bursts and core-collapse supernovae have different environments. *Nature* **2006**, *441*, 463–468, [arXiv:astro-ph/astro-ph/0603537]. <https://doi.org/10.1038/nature04787>.
30. Prochaska, J.X.; Chen, H.W.; Dessauges-Zavadsky, M.; Bloom, J.S. Probing the Interstellar Medium near Star-forming Regions with Gamma-Ray Burst Afterglow Spectroscopy: Gas, Metals, and Dust. *The Astrophysical Journal* **2007**, *666*, 267–280, [arXiv:astro-ph/astro-ph/0703665]. <https://doi.org/10.1086/520042>.
31. Rueda, J.A. An Update of the Binary-Driven Hypernovae Scenario of Long Gamma-Ray Bursts. *Astronomy Reports* **2021**, *65*, 1026–1029. <https://doi.org/10.1134/S1063772921100309>.
32. Woosley, S.E. Gamma-Ray Bursts from Stellar Mass Accretion Disks around Black Holes. *The Astrophysical Journal* **1993**, *405*, 273. <https://doi.org/10.1086/172359>.
33. MacFadyen, A.I.; Woosley, S.E. Collapsars: Gamma-Ray Bursts and Explosions in “Failed Supernovae”. *The Astrophysical Journal* **1999**, *524*, 262–289, [arXiv:astro-ph/astro-ph/9810274]. <https://doi.org/10.1086/307790>.
34. Crowther, P.A. Physical Properties of Wolf-Rayet Stars. *Annual Review of Astronomy and Astrophysics* **2007**, *45*, 177–219, [arXiv:astro-ph/astro-ph/0610356]. <https://doi.org/10.1146/annurev.astro.45.051806.110615>.
35. Bromberg, O.; Nakar, E.; Piran, T.; Sari, R. An Observational Imprint of the Collapsar Model of Long Gamma-Ray Bursts. *The Astrophysical Journal* **2012**, *749*, 110, [arXiv:astro-ph.HE/1111.2990]. <https://doi.org/10.1088/0004-637X/749/2/110>.
36. Kelly, P.L.; Kirshner, R.P.; Pahre, M. Long γ -Ray Bursts and Type Ic Core-Collapse Supernovae Have Similar Locations in Hosts. *The Astrophysical Journal* **2008**, *687*, 1201–1207, [arXiv:astro-ph/0712.0430]. <https://doi.org/10.1086/591925>.
37. Raskin, C.; Scannapieco, E.; Rhoads, J.; Della Valle, M. Using Spatial Distributions to Constrain Progenitors of Supernovae and Gamma-Ray Bursts. *The Astrophysical Journal* **2008**, *689*, 358–370, [arXiv:astro-ph/0808.3766]. <https://doi.org/10.1086/592495>.
38. Berger, E. A Short Gamma-ray Burst “No-host” Problem? Investigating Large Progenitor Offsets for Short GRBs with Optical Afterglows. *The Astrophysical Journal* **2010**, *722*, 1946–1961, [arXiv:astro-ph.HE/1007.0003]. <https://doi.org/10.1088/0004-637X/722/2/1946>.
39. Fong, W.; Berger, E.; Fox, D.B. Hubble Space Telescope Observations of Short Gamma-Ray Burst Host Galaxies: Morphologies, Offsets, and Local Environments. *The Astrophysical Journal* **2010**, *708*, 9–25, [arXiv:astro-ph.HE/0909.1804]. <https://doi.org/10.1088/0004-637X/708/1/9>.
40. Fong, W.; Berger, E. The Locations of Short Gamma-Ray Bursts as Evidence for Compact Object Binary Progenitors. *The Astrophysical Journal* **2013**, *776*, 18, [arXiv:astro-ph.HE/1307.0819]. <https://doi.org/10.1088/0004-637X/776/1/18>.
41. Fong, W.; Berger, E.; Chornock, R.; Margutti, R.; Levan, A.J.; Tanvir, N.R.; Tunnicliffe, R.L.; Czekala, I.; Fox, D.B.; Perley, D.A.; et al. Demographics of the Galaxies Hosting Short-duration Gamma-Ray Bursts. *The Astrophysical Journal* **2013**, *769*, 56, [arXiv:astro-ph.HE/1302.3221]. <https://doi.org/10.1088/0004-637X/769/1/56>.
42. Li, L.X.; Paczyński, B. Transient Events from Neutron Star Mergers. *The Astrophysical Journal* **1998**, *507*, L59–L62, [arXiv:astro-ph/astro-ph/9807272]. <https://doi.org/10.1086/311680>.
43. Tanvir, N.R.; Levan, A.J.; González-Fernández, C.; Korobkin, O.; Mandel, I.; Rosswog, S.; Hjorth, J.; D’Avanzo, P.; Fruchter, A.S.; Fryer, C.L.; et al. The Emergence of a Lanthanide-rich Kilonova Following the Merger of Two Neutron Stars. *The Astrophysical Journal* **2017**, *848*, L27, [arXiv:astro-ph.HE/1710.05455]. <https://doi.org/10.3847/2041-8213/aa90b6>.
44. Smartt, S.J.; Chen, T.W.; Jerkstrand, A.; Coughlin, M.; Kankare, E.; Sim, S.A.; Fraser, M.; Inserra, C.; Maguire, K.; Chambers, K.C.; et al. A kilonova as the electromagnetic counterpart to a gravitational-wave source. *Nature* **2017**, *551*, 75–79, [arXiv:astro-ph.HE/1710.05841]. <https://doi.org/10.1038/nature24303>.
45. Arcavi, I.; Hosseinzadeh, G.; Howell, D.A.; McCully, C.; Poznanski, D.; Kasen, D.; Barnes, J.; Zaltzman, M.; Vasylyev, S.; Maoz, D.; et al. Optical emission from a kilonova following a gravitational-wave-detected neutron-star merger. *Nature* **2017**, *551*, 64–66, [arXiv:astro-ph.HE/1710.05843]. <https://doi.org/10.1038/nature24291>.
46. Metzger, B.D. Kilonovae. *Living Reviews in Relativity* **2017**, *20*, 3, [arXiv:astro-ph.HE/1610.09381]. <https://doi.org/10.1007/s4114-017-0006-z>.
47. Rastinejad, J.C.; Gompertz, B.P.; Levan, A.J.; Fong, W.f.; Nicholl, M.; Lamb, G.P.; Malesani, D.B.; Nugent, A.E.; Oates, S.R.; Tanvir, N.R.; et al. A kilonova following a long-duration gamma-ray burst at 350 Mpc. *Nature* **2022**, *612*, 223–227, [arXiv:astro-ph.HE/2204.10864]. <https://doi.org/10.1038/s41586-022-05390-w>.
48. Yang, J.; Ai, S.; Zhang, B.B.; Zhang, B.; Liu, Z.K.; Wang, X.I.; Yang, Y.H.; Yin, Y.H.; Li, Y.; Lü, H.J. A long-duration gamma-ray burst with a peculiar origin. *Nature* **2022**, *612*, 232–235, [arXiv:astro-ph.HE/2204.12771]. <https://doi.org/10.1038/s41586-022-05403-8>.
49. Chen, M.H.; Li, L.X.; Liang, E.W. Radioactive Gamma-Ray Lines from Long-lived Neutron Star Merger Remnants. *The Astrophysical Journal* **2024**, *971*, 143, [arXiv:astro-ph.HE/2407.14762]. <https://doi.org/10.3847/1538-4357/ad65ec>.
50. Abbott, B.P.; Abbott, R.; Abbott, T.D.; Acernese, F.; Ackley, K.; Adams, C.; Adams, T.; Addesso, P.; Adhikari, R.X.; Adya, V.B.; et al. GW170817: Observation of Gravitational Waves from a Binary Neutron Star Inspiral. *Physical Review Letters* **2017**, *119*, 161101, [arXiv:gr-qc/1710.05832]. <https://doi.org/10.1103/PhysRevLett.119.161101>.
51. Abbott, B.P.; Abbott, R.; Abbott, T.D.; Acernese, F.; Ackley, K.; Adams, C.; Adams, T.; Addesso, P.; Adhikari, R.X.; Adya, V.B.; et al. Multi-messenger Observations of a Binary Neutron Star Merger. *The Astrophysical Journal* **2017**, *848*, L12, [arXiv:astro-ph.HE/1710.05833]. <https://doi.org/10.3847/2041-8213/aa91c9>.

52. Abbott, B.P.; Abbott, R.; Abbott, T.D.; Acernese, F.; Ackley, K.; Adams, C.; Adams, T.; Addesso, P.; Adhikari, R.X.; Adya, V.B.; et al. Gravitational Waves and Gamma-Rays from a Binary Neutron Star Merger: GW170817 and GRB 170817A. *The Astrophysical Journal* **2017**, *848*, L13, [arXiv:astro-ph.HE/1710.05834]. <https://doi.org/10.3847/2041-8213/aa920c>.
53. Rossi, A.; Rothberg, B.; Palazzi, E.; Kann, D.A.; D'Avanzo, P.; Amati, L.; Kloise, S.; Perego, A.; Pian, E.; Guidorzi, C.; et al. The Peculiar Short-duration GRB 200826A and Its Supernova. *The Astrophysical Journal* **2022**, *932*, 1, [arXiv:astro-ph.HE/2105.03829]. <https://doi.org/10.3847/1538-4357/ac60a2>.
54. Bromberg, O.; Nakar, E.; Piran, T.; Sari, R. Short versus Long and Collapsars versus Non-collapsars: A Quantitative Classification of Gamma-Ray Bursts. *The Astrophysical Journal* **2013**, *764*, 179, [arXiv:astro-ph.HE/1210.0068]. <https://doi.org/10.1088/0004-637X/764/2/179>.
55. Horváth, I. A Third Class of Gamma-Ray Bursts? *The Astrophysical Journal* **1998**, *508*, 757–759, [arXiv:astro-ph/astro-ph/9803077]. <https://doi.org/10.1086/306416>.
56. Mukherjee, S.; Feigelson, E.D.; Jogesh Babu, G.; Murtagh, F.; Fraley, C.; Raftery, A. Three Types of Gamma-Ray Bursts. *The Astrophysical Journal* **1998**, *508*, 314–327, [arXiv:astro-ph/astro-ph/9802085]. <https://doi.org/10.1086/306386>.
57. Horváth, I. A further study of the BATSE Gamma-Ray Burst duration distribution. *Astronomy and Astrophysics* **2002**, *392*, 791–793, [arXiv:astro-ph/astro-ph/0205004]. <https://doi.org/10.1051/0004-6361:20020808>.
58. Veres, P.; Bagoly, Z.; Horváth, I.; Mészáros, A.; Balázs, L.G. A Distinct Peak-flux Distribution of the Third Class of Gamma-ray Bursts: A Possible Signature of X-ray Flashes? *The Astrophysical Journal* **2010**, *725*, 1955–1964, [arXiv:astro-ph.HE/1010.2087]. <https://doi.org/10.1088/0004-637X/725/2/1955>.
59. Norris, J.P.; Bonnell, J.T. Short Gamma-Ray Bursts with Extended Emission. *The Astrophysical Journal* **2006**, *643*, 266–275, [arXiv:astro-ph/astro-ph/0601190]. <https://doi.org/10.1086/502796>.
60. Virgili, F.J.; Mundell, C.G.; Pal'shin, V.; Guidorzi, C.; Margutti, R.; Melandri, A.; Harrison, R.; Kobayashi, S.; Chornock, R.; Henden, A.; et al. GRB 091024A and the Nature of Ultra-long Gamma-Ray Bursts. *The Astrophysical Journal* **2013**, *778*, 54, [arXiv:astro-ph.HE/1310.0313]. <https://doi.org/10.1088/0004-637X/778/1/54>.
61. Levan, A.J.; Tanvir, N.R.; Starling, R.L.C.; Wiersema, K.; Page, K.L.; Perley, D.A.; Schulze, S.; Wynn, G.A.; Chornock, R.; Hjorth, J.; et al. A New Population of Ultra-long Duration Gamma-Ray Bursts. *The Astrophysical Journal* **2014**, *781*, 13, [arXiv:astro-ph.HE/1302.2352]. <https://doi.org/10.1088/0004-637X/781/1/13>.
62. Boër, M.; Gendre, B.; Stratta, G. Are Ultra-long Gamma-Ray Bursts Different? *The Astrophysical Journal* **2015**, *800*, 16, [arXiv:astro-ph.HE/1310.4944]. <https://doi.org/10.1088/0004-637X/800/1/16>.
63. Della Valle, M.; Chincarini, G.; Panagia, N.; Tagliaferri, G.; Malesani, D.; Testa, V.; Fugazza, D.; Campana, S.; Covino, S.; Mangano, V.; et al. An enigmatic long-lasting γ -ray burst not accompanied by a bright supernova. *Nature* **2006**, *444*, 1050–1052, [arXiv:astro-ph/astro-ph/0608322]. <https://doi.org/10.1038/nature05374>.
64. Jespersen, C.K.; Severin, J.B.; Steinhardt, C.L.; Vinther, J.; Fynbo, J.P.U.; Selsing, J.; Watson, D. An Unambiguous Separation of Gamma-Ray Bursts into Two Classes from Prompt Emission Alone. *The Astrophysical Journal* **2020**, *896*, L20, [arXiv:astro-ph.HE/2005.13554]. <https://doi.org/10.3847/2041-8213/ab964d>.
65. Garcia-Cifuentes, K.; Becerra, R.L.; De Colle, F.; Cabrera, J.I.; Del Burgo, C. Identification of Extended Emission Gamma-Ray Burst Candidates Using Machine Learning. *The Astrophysical Journal* **2023**, *951*, 4, [arXiv:astro-ph.HE/2304.08666]. <https://doi.org/10.3847/1538-4357/acd176>.
66. Zhang, B. Astrophysics: A burst of new ideas. *Nature* **2006**, *444*, 1010–1011, [arXiv:astro-ph/astro-ph/0612614]. <https://doi.org/10.1038/4441010a>.
67. Kann, D.A.; Kloise, S.; Zhang, B.; Covino, S.; Butler, N.R.; Malesani, D.; Nakar, E.; Wilson, A.C.; Antonelli, L.A.; Chincarini, G.; et al. The Afterglows of Swift-era Gamma-Ray Bursts. II. Type I GRB versus Type II GRB Optical Afterglows. *The Astrophysical Journal* **2011**, *734*, 96, [arXiv:astro-ph/0804.1959]. <https://doi.org/10.1088/0004-637X/734/2/96>.
68. Horváth, I.; Balázs, L.G.; Bagoly, Z.; Ryde, F.; Mészáros, A. A new definition of the intermediate group of gamma-ray bursts. *Astronomy and Astrophysics* **2006**, *447*, 23–30, [arXiv:astro-ph/astro-ph/0509909]. <https://doi.org/10.1051/0004-6361:20041129>.
69. Zhang, B.B.; Burrows, D.N.; Zhang, B.; Mészáros, P.; Wang, X.Y.; Stratta, G.; D'Elia, V.; Frederiks, D.; Golenetskii, S.; Cummings, J.R.; et al. Unusual Central Engine Activity in the Double Burst GRB 110709B. *The Astrophysical Journal* **2012**, *748*, 132, [arXiv:astro-ph.HE/1111.2922]. <https://doi.org/10.1088/0004-637X/748/2/132>.
70. Hu, Y.D.; Liang, E.W.; Xi, S.Q.; Peng, F.K.; Lu, R.J.; Lü, L.Z.; Zhang, B. Internal Energy Dissipation of Gamma-Ray Bursts Observed with Swift: Precursors, Prompt Gamma-Rays, Extended Emission, and Late X-Ray Flares. *The Astrophysical Journal* **2014**, *789*, 145, [arXiv:astro-ph.HE/1405.5949]. <https://doi.org/10.1088/0004-637X/789/2/145>.
71. Lazzati, D. Precursor activity in bright, long BATSE gamma-ray bursts. *Monthly Notices of the Royal Astronomical Society* **2005**, *357*, 722–731, [arXiv:astro-ph/astro-ph/0411753]. <https://doi.org/10.1111/j.1365-2966.2005.08687.x>.
72. Norris, J.P.; Nemiroff, R.J.; Bonnell, J.T.; Scargle, J.D.; Kouveliotou, C.; Paciesas, W.S.; Meegan, C.A.; Fishman, G.J. Attributes of Pulses in Long Bright Gamma-Ray Bursts. *The Astrophysical Journal* **1996**, *459*, 393. <https://doi.org/10.1086/176902>.
73. Norris, J.P.; Bonnell, J.T.; Kazanas, D.; Scargle, J.D.; Hakkila, J.; GIBLIN, T.W. Long-Lag, Wide-Pulse Gamma-Ray Bursts. *The Astrophysical Journal* **2005**, *627*, 324–345, [arXiv:astro-ph/astro-ph/0503383]. <https://doi.org/10.1086/430294>.
74. Band, D.; Matteson, J.; Ford, L.; Schaefer, B.; Palmer, D.; Teegarden, B.; Cline, T.; Briggs, M.; Paciesas, W.; Pendleton, G.; et al. BATSE Observations of Gamma-Ray Burst Spectra. I. Spectral Diversity. *The Astrophysical Journal* **1993**, *413*, 281. <https://doi.org/10.1086/172995>.

75. Preece, R.D.; Briggs, M.S.; Mallozzi, R.S.; Pendleton, G.N.; Paciesas, W.S.; Band, D.L. The BATSE Gamma-Ray Burst Spectral Catalog. I. High Time Resolution Spectroscopy of Bright Bursts Using High Energy Resolution Data. *The Astrophysical Journal Supplement Series* **2000**, *126*, 19–36, [arXiv:astro-ph/9908119]. <https://doi.org/10.1086/313289>.
76. Ryde, F. Is Thermal Emission in Gamma-Ray Bursts Ubiquitous? *The Astrophysical Journal* **2005**, *625*, L95–L98, [arXiv:astro-ph/astro-ph/0504450]. <https://doi.org/10.1086/431239>.
77. Ryde, F.; Pe'er, A. Quasi-blackbody Component and Radiative Efficiency of the Prompt Emission of Gamma-ray Bursts. *The Astrophysical Journal* **2009**, *702*, 1211–1229, [arXiv:astro-ph/0811.4135]. <https://doi.org/10.1088/0004-637X/702/2/1211>.
78. Ryde, F.; Axelsson, M.; Zhang, B.B.; McGlynn, S.; Pe'er, A.; Lundman, C.; Larsson, S.; Battelino, M.; Zhang, B.; Bissaldi, E.; et al. Identification and Properties of the Photospheric Emission in GRB090902B. *The Astrophysical Journal* **2010**, *709*, L172–L177, [arXiv:astro-ph.HE/0911.2025]. <https://doi.org/10.1088/2041-8205/709/2/L172>.
79. Chen, J.M.; Zhu, K.R.; Peng, Z.Y.; Zhang, L. GRB 231129C: Another Thermal Emission Dominated Gamma-Ray Burst. *The Astrophysical Journal* **2024**, *972*, 132. <https://doi.org/10.3847/1538-4357/ad5f93>.
80. Abdo, A.A.; Ackermann, M.; Arimoto, M.; Asano, K.; Atwood, W.B.; Axelsson, M.; Baldini, L.; Ballet, J.; Band, D.L.; Barbiellini, G.; et al. Fermi Observations of High-Energy Gamma-Ray Emission from GRB 080916C. *Science* **2009**, *323*, 1688. <https://doi.org/10.1126/science.1169101>.
81. Abdo, A.A.; Ackermann, M.; Ajello, M.; Asano, K.; Atwood, W.B.; Axelsson, M.; Baldini, L.; Ballet, J.; Barbiellini, G.; Baring, M.G.; et al. Fermi Observations of GRB 090902B: A Distinct Spectral Component in the Prompt and Delayed Emission. *The Astrophysical Journal* **2009**, *706*, L138–L144, [arXiv:astro-ph.HE/0909.2470]. <https://doi.org/10.1088/0004-637X/706/1/L138>.
82. Ackermann, M.; Asano, K.; Atwood, W.B.; Axelsson, M.; Baldini, L.; Ballet, J.; Barbiellini, G.; Baring, M.G.; Bastieri, D.; Bechtol, K.; et al. Fermi Observations of GRB 090510: A Short-Hard Gamma-ray Burst with an Additional, Hard Power-law Component from 10 keV TO GeV Energies. *The Astrophysical Journal* **2010**, *716*, 1178–1190, [arXiv:astro-ph.HE/1005.2141]. <https://doi.org/10.1088/0004-637X/716/2/1178>.
83. Ackermann, M.; Ajello, M.; Asano, K.; Axelsson, M.; Baldini, L.; Ballet, J.; Barbiellini, G.; Baring, M.G.; Bastieri, D.; Bechtol, K.; et al. Detection of a Spectral Break in the Extra Hard Component of GRB 090926A. *The Astrophysical Journal* **2011**, *729*, 114, [arXiv:astro-ph.HE/1101.2082]. <https://doi.org/10.1088/0004-637X/729/2/114>.
84. Golenetskii, S.V.; Mazets, E.P.; Aptekar, R.L.; Ilinskii, V.N. Correlation between luminosity and temperature in γ -ray burst sources. *Nature* **1983**, *306*, 451–453. <https://doi.org/10.1038/306451a0>.
85. Norris, J.P.; Share, G.H.; Messina, D.C.; Dennis, B.R.; Desai, U.D.; Cline, T.L.; Matz, S.M.; Chupp, E.L. Spectral Evolution of Pulse Structures in Gamma-Ray Bursts. *The Astrophysical Journal* **1986**, *301*, 213. <https://doi.org/10.1086/163889>.
86. Lu, R.J.; Wei, J.J.; Liang, E.W.; Zhang, B.B.; Lü, H.J.; Lü, L.Z.; Lei, W.H.; Zhang, B. A Comprehensive Analysis of Fermi Gamma-Ray Burst Data. II. E_p Evolution Patterns and Implications for the Observed Spectrum-Luminosity Relations. *The Astrophysical Journal* **2012**, *756*, 112, [arXiv:astro-ph.HE/1204.0714]. <https://doi.org/10.1088/0004-637X/756/2/112>.
87. Deng, H.Y.; Peng, Z.Y.; Chen, J.M.; Yin, Y.; Li, T. A Study of the Spectral Properties of Gamma-Ray Bursts with the Precursors and Main Bursts. *The Astrophysical Journal* **2024**, *970*, 67, [arXiv:astro-ph.HE/2405.14588]. <https://doi.org/10.3847/1538-4357/ad4d95>.
88. Burrows, D.N.; Romano, P.; Falcone, A.; Kobayashi, S.; Zhang, B.; Moretti, A.; O'Brien, P.T.; Goad, M.R.; Campana, S.; Page, K.L.; et al. Bright X-ray Flares in Gamma-Ray Burst Afterglows. *Science* **2005**, *309*, 1833–1835, [arXiv:astro-ph/astro-ph/0506130]. <https://doi.org/10.1126/science.1116168>.
89. Nousek, J.A.; Kouveliotou, C.; Grupe, D.; Page, K.L.; Granot, J.; Ramirez-Ruiz, E.; Patel, S.K.; Burrows, D.N.; Mangano, V.; Barthelmy, S.; et al. Evidence for a Canonical Gamma-Ray Burst Afterglow Light Curve in the Swift XRT Data. *The Astrophysical Journal* **2006**, *642*, 389–400, [arXiv:astro-ph/astro-ph/0508332]. <https://doi.org/10.1086/500724>.
90. O'Brien, P.T.; Willingale, R.; Osborne, J.; Goad, M.R.; Page, K.L.; Vaughan, S.; Rol, E.; Beardmore, A.; Godet, O.; Hurkett, C.P.; et al. The Early X-Ray Emission from GRBs. *The Astrophysical Journal* **2006**, *647*, 1213–1237, [arXiv:astro-ph/astro-ph/0601125]. <https://doi.org/10.1086/505457>.
91. Zhang, B.; Fan, Y.Z.; Dyks, J.; Kobayashi, S.; Mészáros, P.; Burrows, D.N.; Nousek, J.A.; Gehrels, N. Physical Processes Shaping Gamma-Ray Burst X-Ray Afterglow Light Curves: Theoretical Implications from the Swift X-Ray Telescope Observations. *The Astrophysical Journal* **2006**, *642*, 354–370, [arXiv:astro-ph/astro-ph/0508321]. <https://doi.org/10.1086/500723>.
92. Li, L.; Liang, E.W.; Tang, Q.W.; Chen, J.M.; Xi, S.Q.; Lü, H.J.; Gao, H.; Zhang, B.; Zhang, J.; Yi, S.X.; et al. A Comprehensive Study of Gamma-Ray Burst Optical Emission. I. Flares and Early Shallow-decay Component. *The Astrophysical Journal* **2012**, *758*, 27, [arXiv:astro-ph.HE/1203.2332]. <https://doi.org/10.1088/0004-637X/758/1/27>.
93. Rees, M.J.; Meszaros, P. Relativistic fireballs - Energy conversion and time-scales. *Monthly Notices of the Royal Astronomical Society* **1992**, *258*, 41. <https://doi.org/10.1093/mnras/258.1.41P>.
94. Piran, T.; Shemi, A.; Narayan, R. Hydrodynamics of Relativistic Fireballs. *Monthly Notices of the Royal Astronomical Society* **1993**, *263*, 861, [arXiv:astro-ph/astro-ph/9301004]. <https://doi.org/10.1093/mnras/263.4.861>.
95. Wijers, R.A.M.J.; Rees, M.J.; Meszaros, P. Shocked by GRB 970228: the afterglow of a cosmological fireball. *Monthly Notices of the Royal Astronomical Society* **1997**, *288*, L51–L56, [arXiv:astro-ph/astro-ph/9704153]. <https://doi.org/10.1093/mnras/288.4.L51>.
96. Dai, Z.G.; Lu, T. γ -Ray Bursts and Afterglows from Rotating Strange Stars and Neutron Stars. *Physical Review Letters* **1998**, *81*, 4301–4304, [arXiv:astro-ph/astro-ph/9810332]. <https://doi.org/10.1103/PhysRevLett.81.4301>.

97. Zhang, B.; Mészáros, P. Gamma-Ray Burst Afterglow with Continuous Energy Injection: Signature of a Highly Magnetized Millisecond Pulsar. *The Astrophysical Journal* **2001**, *552*, L35–L38, [arXiv:astro-ph/astro-ph/0011133]. <https://doi.org/10.1086/320255>.
98. Fryer, C.L.; Rueda, J.A.; Ruffini, R. Hypercritical Accretion, Induced Gravitational Collapse, and Binary-Driven Hypernovae. *The Astrophysical Journal* **2014**, *793*, L36, [arXiv:astro-ph.HE/1409.1473]. <https://doi.org/10.1088/2041-8205/793/2/L36>.
99. Fryer, C.L.; Oliveira, F.G.; Rueda, J.A.; Ruffini, R. Neutron-Star-Black-Hole Binaries Produced by Binary-Driven Hypernovae. *Physical Review Letters* **2015**, *115*, 231102, [arXiv:astro-ph.HE/1505.02809]. <https://doi.org/10.1103/PhysRevLett.115.231102>.
100. Rees, M.J.; Meszaros, P. Unsteady Outflow Models for Cosmological Gamma-Ray Bursts. *The Astrophysical Journal* **1994**, *430*, L93, [arXiv:astro-ph/astro-ph/9404038]. <https://doi.org/10.1086/187446>.
101. Kobayashi, S.; Piran, T.; Sari, R. Can Internal Shocks Produce the Variability in Gamma-Ray Bursts? *The Astrophysical Journal* **1997**, *490*, 92, [arXiv:astro-ph/astro-ph/9705013]. <https://doi.org/10.1086/512791>.
102. Daigne, F.; Mochkovitch, R. Gamma-ray bursts from internal shocks in a relativistic wind: temporal and spectral properties. *Monthly Notices of the Royal Astronomical Society* **1998**, *296*, 275–286, [arXiv:astro-ph/astro-ph/9801245]. <https://doi.org/10.1046/j.1365-8711.1998.01305.x>.
103. Geng, J.J.; Huang, Y.F.; Wu, X.F.; Zhang, B.; Zong, H.S. Low-energy Spectra of Gamma-Ray Bursts from Cooling Electrons. *The Astrophysical Journal Supplement Series* **2018**, *234*, 3, [arXiv:astro-ph.HE/1709.05899]. <https://doi.org/10.3847/1538-4365/aa9e84>.
104. Pe’er, A.; Ryde, F. A Theory of Multicolor Blackbody Emission from Relativistically Expanding Plasmas. *The Astrophysical Journal* **2011**, *732*, 49, [arXiv:astro-ph.HE/1008.4590]. <https://doi.org/10.1088/0004-637X/732/1/49>.
105. Bhattacharya, M.; Kumar, P. Explaining GRB prompt emission with sub-photospheric dissipation and Comptonization. *Monthly Notices of the Royal Astronomical Society* **2020**, *491*, 4656–4671, [arXiv:astro-ph.HE/1909.07398]. <https://doi.org/10.1093/mnras/stz3182>.
106. Sari, R.; Piran, T.; Narayan, R. Spectra and Light Curves of Gamma-Ray Burst Afterglows. *The Astrophysical Journal* **1998**, *497*, L17–L20, [arXiv:astro-ph/astro-ph/9712005]. <https://doi.org/10.1086/311269>.
107. Preece, R.D.; Briggs, M.S.; Mallozzi, R.S.; Pendleton, G.N.; Paciesas, W.S.; Band, D.L. The Synchrotron Shock Model Confronts a “Line of Death” in the BATSE Gamma-Ray Burst Data. *The Astrophysical Journal* **1998**, *506*, L23–L26, [arXiv:astro-ph/astro-ph/9808184]. <https://doi.org/10.1086/311644>.
108. Nava, L.; Ghirlanda, G.; Ghisellini, G.; Celotti, A. Spectral properties of 438 GRBs detected by Fermi/GBM. *Astronomy and Astrophysics* **2011**, *530*, A21, [arXiv:astro-ph.HE/1012.2863]. <https://doi.org/10.1051/0004-6361/201016270>.
109. Nava, L.; Ghirlanda, G.; Ghisellini, G.; Celotti, A. Fermi/GBM and BATSE gamma-ray bursts: comparison of the spectral properties. *Monthly Notices of the Royal Astronomical Society* **2011**, *415*, 3153–3162, [arXiv:astro-ph.HE/1012.3968]. <https://doi.org/10.1111/j.1365-2966.2011.18928.x>.
110. Blandford, R.D.; McKee, C.F. Fluid dynamics of relativistic blast waves. *Physics of Fluids* **1976**, *19*, 1130–1138. <https://doi.org/10.1063/1.861619>.
111. Ioka, K.; Toma, K.; Yamazaki, R.; Nakamura, T. Efficiency crisis of swift gamma-ray bursts with shallow X-ray afterglows: prior activity or time-dependent microphysics? *Astronomy and Astrophysics* **2006**, *458*, 7–12, [arXiv:astro-ph/astro-ph/0511749]. <https://doi.org/10.1051/0004-6361:20064939>.
112. Racusin, J.L.; Karpov, S.V.; Sokolowski, M.; Granot, J.; Wu, X.F.; Pal’Shin, V.; Covino, S.; van der Horst, A.J.; Oates, S.R.; Schady, P.; et al. Broadband observations of the naked-eye γ -ray burst GRB080319B. *Nature* **2008**, *455*, 183–188, [arXiv:astro-ph/0805.1557]. <https://doi.org/10.1038/nature07270>.
113. Dereli-Bégué, H.; Pe’er, A.; Ryde, F.; Oates, S.R.; Zhang, B.; Dainotti, M.G. A wind environment and Lorentz factors of tens explain gamma-ray bursts X-ray plateau. *Nature Communications* **2022**, *13*, 5611, [arXiv:astro-ph.HE/2207.11066]. <https://doi.org/10.1038/s41467-022-32881-1>.
114. Oganessian, G.; Ascenzi, S.; Branchesi, M.; Salafia, O.S.; Dall’Osso, S.; Ghirlanda, G. Structured Jets and X-Ray Plateaus in Gamma-Ray Burst Phenomena. *The Astrophysical Journal* **2020**, *893*, 88, [arXiv:astro-ph.HE/1904.08786]. <https://doi.org/10.3847/1538-4357/ab8221>.
115. Cucchiara, A.; Levan, A.J.; Fox, D.B.; Tanvir, N.R.; Ukwatta, T.N.; Berger, E.; Krühler, T.; Küpcü Yoldaş, A.; Wu, X.F.; Toma, K.; et al. A Photometric Redshift of $z \sim 9.4$ for GRB 090429B. *The Astrophysical Journal* **2011**, *736*, 7, [arXiv:astro-ph.CO/1105.4915]. <https://doi.org/10.1088/0004-637X/736/1/7>.
116. Salvaterra, R.; Della Valle, M.; Campana, S.; Chincarini, G.; Covino, S.; D’Avanzo, P.; Fernández-Soto, A.; Guidorzi, C.; Mannucci, F.; Margutti, R.; et al. GRB090423 at a redshift of $z \sim 8.1$. *Nature* **2009**, *461*, 1258–1260, [arXiv:astro-ph.CO/0906.1578]. <https://doi.org/10.1038/nature08445>.
117. Wang, F.Y.; Dai, Z.G.; Liang, E.W. Gamma-ray burst cosmology. *New Astronomy Reviews* **2015**, *67*, 1–17, [arXiv:astro-ph.HE/1504.00735]. <https://doi.org/10.1016/j.newar.2015.03.001>.
118. Dainotti, M.G.; Del Vecchio, R. Gamma Ray Burst afterglow and prompt-afterglow relations: An overview. *New Astronomy Reviews* **2017**, *77*, 23–61, [arXiv:astro-ph.HE/1703.06876]. <https://doi.org/10.1016/j.newar.2017.04.001>.
119. Dainotti, M.G.; Del Vecchio, R.; Tarnopolski, M. Gamma-Ray Burst Prompt Correlations. *Advances in Astronomy* **2018**, *2018*, 4969503, [arXiv:astro-ph.HE/1612.00618]. <https://doi.org/10.1155/2018/4969503>.
120. Dainotti, M. *Gamma-ray Burst Correlations; Current status and open questions*; 2019. <https://doi.org/10.1088/2053-2563/aae15c>.

121. Parsotan, T.; Ito, H. GRB Prompt Emission: Observed Correlations and Their Interpretations. *Universe* **2022**, *8*, 310, [arXiv:astro-ph.HE/2204.09729]. <https://doi.org/10.3390/universe8060310>.
122. Norris, J.P.; Marani, G.F.; Bonnell, J.T. Connection between Energy-dependent Lags and Peak Luminosity in Gamma-Ray Bursts. *The Astrophysical Journal* **2000**, *534*, 248–257, [arXiv:astro-ph/astro-ph/9903233]. <https://doi.org/10.1086/308725>.
123. Schaefer, B.E.; Deng, M.; Band, D.L. Redshifts and Luminosities for 112 Gamma-Ray Bursts. *The Astrophysical Journal* **2001**, *563*, L123–L127, [arXiv:astro-ph/astro-ph/0101461]. <https://doi.org/10.1086/338651>.
124. Tsutsui, R.; Nakamura, T.; Yonetoku, D.; Murakami, T.; Tanabe, S.; Kodama, Y. Redshift-dependent lag-luminosity relation in 565 BATSE gamma-ray bursts. *Monthly Notices of the Royal Astronomical Society* **2008**, *386*, L33–L37. <https://doi.org/10.1111/j.1745-3933.2008.00455.x>.
125. Ukwatta, T.N.; Dhuga, K.S.; Stamatikos, M.; Dermer, C.D.; Sakamoto, T.; Sonbas, E.; Parke, W.C.; Maximon, L.C.; Linnemann, J.T.; Bhat, P.N.; et al. The lag-luminosity relation in the GRB source frame: an investigation with Swift BAT bursts. *Monthly Notices of the Royal Astronomical Society* **2012**, *419*, 614–623, [arXiv:astro-ph.HE/1109.0666]. <https://doi.org/10.1111/j.1365-2966.2011.19723.x>.
126. Margutti, R.; Guidorzi, C.; Chincarini, G.; Bernardini, M.G.; Genet, F.; Mao, J.; Pasotti, F. Lag-luminosity relation in γ -ray burst X-ray flares: a direct link to the prompt emission. *Monthly Notices of the Royal Astronomical Society* **2010**, *406*, 2149–2167, [arXiv:astro-ph.HE/1004.1568]. <https://doi.org/10.1111/j.1365-2966.2010.16824.x>.
127. Salmonson, J.D. On the Kinematic Origin of the Luminosity-Pulse Lag Relationship in Gamma-Ray Bursts. *The Astrophysical Journal* **2000**, *544*, L115–L117, [arXiv:astro-ph/astro-ph/0005264]. <https://doi.org/10.1086/317305>.
128. Schaefer, B.E. Explaining the Gamma-Ray Burst Lag/Luminosity Relation. *The Astrophysical Journal* **2004**, *602*, 306–311. <https://doi.org/10.1086/380898>.
129. Chen, Y.; Liu, R.Y.; Wang, X.Y. Constraints on the bulk Lorentz factor of gamma-ray bursts with the detection rate by Fermi LAT. *Monthly Notices of the Royal Astronomical Society* **2018**, *478*, 749–757. <https://doi.org/10.1093/mnras/sty1171>.
130. Ghirlanda, G.; Nappo, F.; Ghisellini, G.; Melandri, A.; Marcarini, G.; Nava, L.; Salafia, O.S.; Campana, S.; Salvaterra, R. Bulk Lorentz factors of gamma-ray bursts. *Astronomy and Astrophysics* **2018**, *609*, A112, [arXiv:astro-ph.HE/1711.06257]. <https://doi.org/10.1051/0004-6361/201731598>.
131. Ioka, K.; Nakamura, T. Peak Luminosity-Spectral Lag Relation Caused by the Viewing Angle of the Collimated Gamma-Ray Bursts. *The Astrophysical Journal* **2001**, *554*, L163–L167, [arXiv:astro-ph/astro-ph/0105321]. <https://doi.org/10.1086/321717>.
132. Shen, R.F.; Song, L.M.; Li, Z. Spectral lags and the energy dependence of pulse width in gamma-ray bursts: contributions from the relativistic curvature effect. *Monthly Notices of the Royal Astronomical Society* **2005**, *362*, 59–65, [arXiv:astro-ph/astro-ph/0505276]. <https://doi.org/10.1111/j.1365-2966.2005.09163.x>.
133. Lu, R.J.; Qin, Y.P.; Zhang, Z.B.; Yi, T.F. Spectral lags caused by the curvature effect of fireballs. *Monthly Notices of the Royal Astronomical Society* **2006**, *367*, 275–289, [arXiv:astro-ph/astro-ph/0509287]. <https://doi.org/10.1111/j.1365-2966.2005.09951.x>.
134. Reichart, D.E.; Lamb, D.Q.; Fenimore, E.E.; Ramirez-Ruiz, E.; Cline, T.L.; Hurley, K. A Possible Cepheid-like Luminosity Estimator for the Long Gamma-Ray Bursts. *The Astrophysical Journal* **2001**, *552*, 57–71, [arXiv:astro-ph/astro-ph/0004302]. <https://doi.org/10.1086/320434>.
135. Fenimore, E.E.; Ramirez-Ruiz, E. Redshifts For 220 BATSE Gamma-Ray Bursts Determined by Variability and the Cosmological Consequences. *arXiv e-prints* **2000**, pp. astro-ph/0004176, [arXiv:astro-ph/astro-ph/0004176]. <https://doi.org/10.48550/arXiv.astro-ph/0004176>.
136. Guidorzi, C.; Frontera, F.; Montanari, E.; Rossi, F.; Amati, L.; Gomboc, A.; Hurley, K.; Mundell, C.G. The gamma-ray burst variability-peak luminosity correlation: new results. *Monthly Notices of the Royal Astronomical Society* **2005**, *363*, 315–325, [arXiv:astro-ph/astro-ph/0507588]. <https://doi.org/10.1111/j.1365-2966.2005.09450.x>.
137. Reichart, D.E.; Nysewander, M.C. GRB Variability-Luminosity Correlation Confirmed. *arXiv e-prints* **2005**, pp. astro-ph/0508111, [arXiv:astro-ph/astro-ph/0508111]. <https://doi.org/10.48550/arXiv.astro-ph/0508111>.
138. Guidorzi, C.; Frontera, F.; Montanari, E.; Rossi, F.; Amati, L.; Gomboc, A.; Mundell, C.G. The slope of the gamma-ray burst variability/peak luminosity correlation. *Monthly Notices of the Royal Astronomical Society* **2006**, *371*, 843–851, [arXiv:astro-ph/astro-ph/0606526]. <https://doi.org/10.1111/j.1365-2966.2006.10717.x>.
139. Li, L.X.; Paczyński, B. Improved correlation between the variability and peak luminosity of gamma-ray bursts. *Monthly Notices of the Royal Astronomical Society* **2006**, *366*, 219–226, [arXiv:astro-ph/astro-ph/0509776]. <https://doi.org/10.1111/j.1365-2966.2005.09836.x>.
140. Rizzuto, D.; Guidorzi, C.; Romano, P.; Covino, S.; Campana, S.; Capalbi, M.; Chincarini, G.; Cusumano, G.; Fugazza, D.; Mangano, V.; et al. Testing the gamma-ray burst variability/peak luminosity correlation on a Swift homogeneous sample. *Monthly Notices of the Royal Astronomical Society* **2007**, *379*, 619–628, [arXiv:astro-ph/0704.2486]. <https://doi.org/10.1111/j.1365-2966.2007.11880.x>.
141. Guidorzi, C.; Maccary, R.; Tsvetkova, A.; Kobayashi, S.; Amati, L.; Bazzanini, L.; Bulla, M.; Camisasca, A.E.; Ferro, L.; Frederiks, D.; et al. New results on the gamma-ray burst variability–luminosity relation. *Astronomy and Astrophysics* **2024**, *690*, A261, [arXiv:astro-ph.HE/2409.01644]. <https://doi.org/10.1051/0004-6361/202451401>.
142. Camisasca, A.E.; Guidorzi, C.; Amati, L.; Frontera, F.; Song, X.Y.; Xiao, S.; Xiong, S.L.; Zhang, S.N.; Margutti, R.; Kobayashi, S.; et al. GRB minimum variability timescale with Insight-HXMT and Swift. Implications for progenitor models, dissipation physics, and GRB classifications. *Astronomy and Astrophysics* **2023**, *671*, A112, [arXiv:astro-ph.HE/2301.01176]. <https://doi.org/10.1051/0004-6361/202245657>.

143. Schaefer, B.E. The Hubble Diagram to Redshift >6 from 69 Gamma-Ray Bursts. *The Astrophysical Journal* **2007**, *660*, 16–46, [arXiv:astro-ph/astro-ph/0612285]. <https://doi.org/10.1086/511742>.
144. Salmonson, J.D.; Galama, T.J. Discovery of a Tight Correlation between Pulse Lag/Luminosity and Jet-Break Times: A Connection between Gamma-Ray Bursts and Afterglow Properties. *The Astrophysical Journal* **2002**, *569*, 682–688, [arXiv:astro-ph/astro-ph/0112298]. <https://doi.org/10.1086/339391>.
145. Kobayashi, S.; Ryde, F.; MacFadyen, A. Luminosity and Variability of Collimated Gamma-Ray Bursts. *The Astrophysical Journal* **2002**, *577*, 302–310, [arXiv:astro-ph/astro-ph/0110080]. <https://doi.org/10.1086/342123>.
146. Mészáros, P.; Ramirez-Ruiz, E.; Rees, M.J.; Zhang, B. X-Ray-rich Gamma-Ray Bursts, Photospheres, and Variability. *The Astrophysical Journal* **2002**, *578*, 812–817, [arXiv:astro-ph/astro-ph/0205144]. <https://doi.org/10.1086/342611>.
147. Salafia, O.S.; Ghisellini, G.; Pescalli, A.; Ghirlanda, G.; Nappo, F. Light curves and spectra from off-axis gamma-ray bursts. *Monthly Notices of the Royal Astronomical Society* **2016**, *461*, 3607–3619, [arXiv:astro-ph.HE/1601.03735]. <https://doi.org/10.1093/mnras/stw1549>.
148. Amati, L.; Frontera, F.; Tavani, M.; in't Zand, J.J.M.; Antonelli, A.; Costa, E.; Feroci, M.; Guidorzi, C.; Heise, J.; Masetti, N.; et al. Intrinsic spectra and energetics of BeppoSAX Gamma-Ray Bursts with known redshifts. *Astronomy and Astrophysics* **2002**, *390*, 81–89, [arXiv:astro-ph/astro-ph/0205230]. <https://doi.org/10.1051/0004-6361:20020722>.
149. Lamb, D.Q.; Donaghy, T.Q.; Graziani, C. A unified jet model of X-ray flashes and γ -ray bursts. *New Astronomy Reviews* **2004**, *48*, 459–464, [arXiv:astro-ph/astro-ph/0309456]. <https://doi.org/10.1016/j.newar.2003.12.030>.
150. Sakamoto, T.; Lamb, D.Q.; Graziani, C.; Donaghy, T.Q.; Suzuki, M.; Ricker, G.; Atteia, J.L.; Kawai, N.; Yoshida, A.; Shirasaki, Y.; et al. High Energy Transient Explorer 2 Observations of the Extremely Soft X-Ray Flash XRF 020903. *The Astrophysical Journal* **2004**, *602*, 875–885. <https://doi.org/10.1086/381232>.
151. Amati, L.; Guidorzi, C.; Frontera, F.; Della Valle, M.; Finelli, F.; Landi, R.; Montanari, E. Measuring the cosmological parameters with the $E_{p,i}$ - E_{iso} correlation of gamma-ray bursts. *Monthly Notices of the Royal Astronomical Society* **2008**, *391*, 577–584, [arXiv:astro-ph/0805.0377]. <https://doi.org/10.1111/j.1365-2966.2008.13943.x>.
152. Amati, L. COSMOLOGY WITH THE $E_{p,i}$ - E_{iso} CORRELATION OF GAMMA-RAY BURSTS. In Proceedings of the International Journal of Modern Physics Conference Series, 2012, Vol. 12, *International Journal of Modern Physics Conference Series*, pp. 19–27. <https://doi.org/10.1142/S2010194512006228>.
153. Amati, L.; Della Valle, M. Measuring Cosmological Parameters with Gamma Ray Bursts. *International Journal of Modern Physics D* **2013**, *22*, 1330028, [arXiv:astro-ph.CO/1310.3141]. <https://doi.org/10.1142/S0218271813300280>.
154. Geng, J.J.; Huang, Y.F. On the Correlation of Low-energy Spectral Indices and Redshifts of Gamma-Ray Bursts. *The Astrophysical Journal* **2013**, *764*, 75, [arXiv:astro-ph.HE/1212.4340]. <https://doi.org/10.1088/0004-637X/764/1/75>.
155. Demianski, M.; Piedipalumbo, E.; Sawant, D.; Amati, L. Cosmology with gamma-ray bursts. I. The Hubble diagram through the calibrated $E_{p,i}$ - E_{iso} correlation. *Astronomy and Astrophysics* **2017**, *598*, A112, [arXiv:astro-ph.CO/1610.00854]. <https://doi.org/10.1051/0004-6361/201628909>.
156. Nava, L.; Salvaterra, R.; Ghirlanda, G.; Ghisellini, G.; Campana, S.; Covino, S.; Cusumano, G.; D'Avanzo, P.; D'Elia, V.; Fugazza, D.; et al. A complete sample of bright Swift long gamma-ray bursts: testing the spectral-energy correlations. *Monthly Notices of the Royal Astronomical Society* **2012**, *421*, 1256–1264, [arXiv:astro-ph.HE/1112.4470]. <https://doi.org/10.1111/j.1365-2966.2011.20394.x>.
157. Basak, R.; Rao, A.R. Correlation between the Isotropic Energy and the Peak Energy at Zero Fluence for the Individual Pulses of Gamma-Ray Bursts: Toward a Universal Physical Correlation for the Prompt Emission. *The Astrophysical Journal* **2012**, *749*, 132, [arXiv:astro-ph.HE/1202.3089]. <https://doi.org/10.1088/0004-637X/749/2/132>.
158. Basak, R.; Rao, A.R. Pulse-wise Amati correlation in Fermi gamma-ray bursts. *Monthly Notices of the Royal Astronomical Society* **2013**, *436*, 3082–3088, [arXiv:astro-ph.HE/1309.5233]. <https://doi.org/10.1093/mnras/stt1790>.
159. Thompson, C.; Mészáros, P.; Rees, M.J. Thermalization in Relativistic Outflows and the Correlation between Spectral Hardness and Apparent Luminosity in Gamma-Ray Bursts. *The Astrophysical Journal* **2007**, *666*, 1012–1023, [arXiv:astro-ph/astro-ph/0608282]. <https://doi.org/10.1086/518551>.
160. Pe'er, A.; Mészáros, P.; Rees, M.J. The Observable Effects of a Photospheric Component on GRB and XRF Prompt Emission Spectrum. *The Astrophysical Journal* **2006**, *642*, 995–1003, [arXiv:astro-ph/astro-ph/0510114]. <https://doi.org/10.1086/501424>.
161. Giannios, D.; Spruit, H.C. Spectral and timing properties of a dissipative γ -ray burst photosphere. *Astronomy and Astrophysics* **2007**, *469*, 1–9, [arXiv:astro-ph/astro-ph/0611385]. <https://doi.org/10.1051/0004-6361:20066739>.
162. Giannios, D. The peak energy of dissipative gamma-ray burst photospheres. *Monthly Notices of the Royal Astronomical Society* **2012**, *422*, 3092–3098, [arXiv:astro-ph.HE/1111.4258]. <https://doi.org/10.1111/j.1365-2966.2012.20825.x>.
163. Eichler, D.; Levinson, A. An Interpretation of the $h\nu_{peak}$ - E_{iso} Correlation for Gamma-Ray Bursts. *The Astrophysical Journal* **2004**, *614*, L13–L16, [arXiv:astro-ph/astro-ph/0405014]. <https://doi.org/10.1086/425310>.
164. Dado, S.; Dar, A. Kinematic Origin of Correlations between Gamma-Ray Burst Observables. *The Astrophysical Journal* **2012**, *749*, 100, [arXiv:astro-ph.HE/1001.1865]. <https://doi.org/10.1088/0004-637X/749/2/100>.
165. Yamazaki, R.; Ioka, K.; Nakamura, T. Peak Energy-Isotropic Energy Relation in the Off-Axis Gamma-Ray Burst Model. *The Astrophysical Journal* **2004**, *606*, L33–L36, [arXiv:astro-ph/astro-ph/0401044]. <https://doi.org/10.1086/421084>.
166. Kocevski, D. On the Origin of High-energy Correlations in Gamma-Ray Bursts. *The Astrophysical Journal* **2012**, *747*, 146, [arXiv:astro-ph.HE/1110.6173]. <https://doi.org/10.1088/0004-637X/747/2/146>.

167. Mochkovitch, R.; Nava, L. The $E_p - E_{iso}$ relation and the internal shock model. *Astronomy and Astrophysics* **2015**, *577*, A31, [arXiv:astro-ph.HE/1412.5807]. <https://doi.org/10.1051/0004-6361/201424490>.
168. Heussaff, V.; Atteia, J.L.; Zolnierowski, Y. The $E_{peak} - E_{iso}$ relation revisited with Fermi GRBs. Resolving a long-standing debate? *Astronomy and Astrophysics* **2013**, *557*, A100, [arXiv:astro-ph.HE/1306.1757]. <https://doi.org/10.1051/0004-6361/201321528>.
169. Stanway, E.R.; Levan, A.J.; Tanvir, N.; Wiersema, K.; van der Horst, A.; Mundell, C.G.; Guidorzi, C. GRB 080517: a local, low-luminosity gamma-ray burst in a dusty galaxy at $z = 0.09$. *Monthly Notices of the Royal Astronomical Society* **2015**, *446*, 3911–3925, [arXiv:astro-ph.GA/1409.5791]. <https://doi.org/10.1093/mnras/stu2286>.
170. D’Elia, V.; Campana, S.; D’Ai, A.; De Pasquale, M.; Emery, S.W.K.; Frederiks, D.D.; Lien, A.; Melandri, A.; Page, K.L.; Starling, R.L.C.; et al. GRB 171205A/SN 2017iuk: A local low-luminosity gamma-ray burst. *Astronomy and Astrophysics* **2018**, *619*, A66, [arXiv:astro-ph.HE/1810.03339]. <https://doi.org/10.1051/0004-6361/201833847>.
171. Farinelli, R.; Basak, R.; Amati, L.; Guidorzi, C.; Frontera, F. A numerical jet model for the prompt emission of gamma-ray bursts. *Monthly Notices of the Royal Astronomical Society* **2021**, *501*, 5723–5732, [arXiv:astro-ph.HE/2101.02984]. <https://doi.org/10.1093/mnras/staa4048>.
172. Xu, F.; Huang, Y.F.; Geng, J.J.; Wu, X.F.; Li, X.J.; Zhang, Z.B. An analytic derivation of the empirical correlations of gamma-ray bursts. *Astronomy and Astrophysics* **2023**, *673*, A20, [arXiv:astro-ph.HE/2211.04727]. <https://doi.org/10.1051/0004-6361/202245414>.
173. Yonetoku, D.; Murakami, T.; Nakamura, T.; Yamazaki, R.; Inoue, A.K.; Ioka, K. Gamma-Ray Burst Formation Rate Inferred from the Spectral Peak Energy-Peak Luminosity Relation. *The Astrophysical Journal* **2004**, *609*, 935–951, [arXiv:astro-ph/astro-ph/0309217]. <https://doi.org/10.1086/421285>.
174. Ghirlanda, G.; Ghisellini, G.; Celotti, A. The spectra of short gamma-ray bursts. *Astronomy and Astrophysics* **2004**, *422*, L55–L58, [arXiv:astro-ph/astro-ph/0310861]. <https://doi.org/10.1051/0004-6361:20048008>.
175. Ghirlanda, G.; Nava, L.; Ghisellini, G.; Celotti, A.; Firmani, C. Short versus long gamma-ray bursts: spectra, energetics, and luminosities. *Astronomy and Astrophysics* **2009**, *496*, 585–595, [arXiv:astro-ph.HE/0902.0983]. <https://doi.org/10.1051/0004-6361/200811209>.
176. Zhang, B.; Zhang, B.B.; Virgili, F.J.; Liang, E.W.; Kann, D.A.; Wu, X.F.; Proga, D.; Lv, H.J.; Toma, K.; Mészáros, P.; et al. Discerning the Physical Origins of Cosmological Gamma-ray Bursts Based on Multiple Observational Criteria: The Cases of $z = 6.7$ GRB 080913, $z = 8.2$ GRB 090423, and Some Short/Hard GRBs. *The Astrophysical Journal* **2009**, *703*, 1696–1724, [arXiv:astro-ph.HE/0902.2419]. <https://doi.org/10.1088/0004-637X/703/2/1696>.
177. Zhang, Z.B.; Chen, D.Y.; Huang, Y.F. Correlation between Peak Energy and Peak Luminosity in Short Gamma-Ray Bursts. *The Astrophysical Journal* **2012**, *755*, 55, [arXiv:astro-ph.CO/1205.2411]. <https://doi.org/10.1088/0004-637X/755/1/55>.
178. Shahmoradi, A.; Nemiroff, R.J. Short versus long gamma-ray bursts: a comprehensive study of energetics and prompt gamma-ray correlations. *Monthly Notices of the Royal Astronomical Society* **2015**, *451*, 126–143, [arXiv:astro-ph.HE/1412.5630]. <https://doi.org/10.1093/mnras/stv714>.
179. D’Avanzo, P.; Salvaterra, R.; Bernardini, M.G.; Nava, L.; Campana, S.; Covino, S.; D’Elia, V.; Ghirlanda, G.; Ghisellini, G.; Melandri, A.; et al. A complete sample of bright Swift short gamma-ray bursts. *Monthly Notices of the Royal Astronomical Society* **2014**, *442*, 2342–2356, [arXiv:astro-ph.HE/1405.5131]. <https://doi.org/10.1093/mnras/stu994>.
180. Tsutsui, R.; Yonetoku, D.; Nakamura, T.; Takahashi, K.; Morihara, Y. Possible existence of the $E_p - L_p$ and $E_p - E_{iso}$ correlations for short gamma-ray bursts with a factor 5–100 dimmer than those for long gamma-ray bursts. *Monthly Notices of the Royal Astronomical Society* **2013**, *431*, 1398–1404, [arXiv:astro-ph.HE/1208.0429]. <https://doi.org/10.1093/mnras/stt262>.
181. Yonetoku, D.; Murakami, T.; Tsutsui, R.; Nakamura, T.; Morihara, Y.; Takahashi, K. Possible Origins of Dispersion of the Peak Energy-Brightness Correlations of Gamma-Ray Bursts. *Publications of the Astronomical Society of Japan* **2010**, *62*, 1495, [arXiv:astro-ph.HE/1201.2745]. <https://doi.org/10.1093/pasj/62.6.1495>.
182. Nakar, E.; Piran, T. Outliers to the peak energy-isotropic energy relation in gamma-ray bursts. *Monthly Notices of the Royal Astronomical Society* **2005**, *360*, L73–L76, [arXiv:astro-ph/astro-ph/0412232]. <https://doi.org/10.1111/j.1745-3933.2005.00049.x>.
183. Band, D.L.; Preece, R.D. Testing the Gamma-Ray Burst Energy Relationships. *The Astrophysical Journal* **2005**, *627*, 319–323, [arXiv:astro-ph/astro-ph/0501559]. <https://doi.org/10.1086/430402>.
184. Butler, N.R.; Kocevski, D.; Bloom, J.S.; Curtis, J.L. A Complete Catalog of Swift Gamma-Ray Burst Spectra and Durations: Demise of a Physical Origin for Pre-Swift High-Energy Correlations. *The Astrophysical Journal* **2007**, *671*, 656–677, [arXiv:astro-ph/0706.1275]. <https://doi.org/10.1086/522492>.
185. Ito, H.; Nagataki, S.; Matsumoto, J.; Lee, S.H.; Tolstov, A.; Mao, J.; Dainotti, M.; Mizuta, A. Spectral and Polarization Properties of Photospheric Emission from Stratified Jets. *The Astrophysical Journal* **2014**, *789*, 159, [arXiv:astro-ph.HE/1405.6284]. <https://doi.org/10.1088/0004-637X/789/2/159>.
186. Ito, H.; Just, O.; Takei, Y.; Nagataki, S. A Global Numerical Model of the Prompt Emission in Short Gamma-ray Bursts. *The Astrophysical Journal* **2021**, *918*, 59, [arXiv:astro-ph.HE/2105.09323]. <https://doi.org/10.3847/1538-4357/ac0cf9>.
187. Ito, H.; Matsumoto, J.; Nagataki, S.; Warren, D.C.; Barkov, M.V.; Yonetoku, D. Numerical Simulation of Photospheric Emission in Long Gamma-Ray Bursts: Prompt Correlations, Spectral Shapes, and Polarizations. *The Astrophysical Journal* **2024**, *961*, 243, [arXiv:astro-ph.HE/2307.10023]. <https://doi.org/10.3847/1538-4357/ace775>.

188. Fan, Y.Z.; Wei, D.M.; Zhang, F.W.; Zhang, B.B. The Photospheric Radiation Model for the Prompt Emission of Gamma-Ray Bursts: Interpreting Four Observed Correlations. *The Astrophysical Journal* **2012**, *755*, L6, [arXiv:astro-ph.HE/1204.4881]. <https://doi.org/10.1088/2041-8205/755/1/L6>.
189. Ito, H.; Matsumoto, J.; Nagataki, S.; Warren, D.C.; Barkov, M.V.; Yonetoku, D. The photospheric origin of the Yonetoku relation in gamma-ray bursts. *Nature Communications* **2019**, *10*, 1504, [arXiv:astro-ph.HE/1806.00590]. <https://doi.org/10.1038/s41467-019-09281-z>.
190. Dainotti, M.G.; Cardone, V.F.; Capozziello, S. A time-luminosity correlation for γ -ray bursts in the X-rays. *Monthly Notices of the Royal Astronomical Society* **2008**, *391*, L79–L83, [arXiv:astro-ph/0809.1389]. <https://doi.org/10.1111/j.1745-3933.2008.00560.x>.
191. Bloom, J.S.; Frail, D.A.; Sari, R. The Prompt Energy Release of Gamma-Ray Bursts using a Cosmological k-Correction. *The Astronomical Journal* **2001**, *121*, 2879–2888, [arXiv:astro-ph/astro-ph/0102371]. <https://doi.org/10.1086/321093>.
192. Willingale, R.; O'Brien, P.T.; Osborne, J.P.; Godet, O.; Page, K.L.; Goad, M.R.; Burrows, D.N.; Zhang, B.; Rol, E.; Gehrels, N.; et al. Testing the Standard Fireball Model of Gamma-Ray Bursts Using Late X-Ray Afterglows Measured by Swift. *The Astrophysical Journal* **2007**, *662*, 1093–1110, [arXiv:astro-ph/astro-ph/0612031]. <https://doi.org/10.1086/517989>.
193. Dainotti, M.G.; Willingale, R.; Capozziello, S.; Fabrizio Cardone, V.; Ostrowski, M. Discovery of a Tight Correlation for Gamma-ray Burst Afterglows with “Canonical” Light Curves. *The Astrophysical Journal* **2010**, *722*, L215–L219, [arXiv:astro-ph.HE/1009.1663]. <https://doi.org/10.1088/2041-8205/722/2/L215>.
194. Cardone, V.F.; Dainotti, M.G.; Capozziello, S.; Willingale, R. Constraining cosmological parameters by gamma-ray burst X-ray afterglow light curves. *Monthly Notices of the Royal Astronomical Society* **2010**, *408*, 1181–1186, [arXiv:astro-ph.CO/1005.0122]. <https://doi.org/10.1111/j.1365-2966.2010.17197.x>.
195. Sultana, J.; Kazanas, D.; Fukumura, K. Luminosity Correlations for Gamma-Ray Bursts and Implications for Their Prompt and Afterglow Emission Mechanisms. *The Astrophysical Journal* **2012**, *758*, 32, [arXiv:astro-ph.HE/1208.1680]. <https://doi.org/10.1088/0004-637X/758/1/32>.
196. Bernardini, M.G.; Margutti, R.; Mao, J.; Zaninoni, E.; Chincarini, G. The X-ray light curve of gamma-ray bursts: clues to the central engine. *Astronomy and Astrophysics* **2012**, *539*, A3, [arXiv:astro-ph.HE/1112.1058]. <https://doi.org/10.1051/0004-6361/201117895>.
197. Mangano, V.; Sbarufatti, B.; Stratta, G. Extending the plateau luminosity-duration anticorrelation. *Memorie della Societa Astronomica Italiana Supplementi* **2012**, *21*, 143.
198. Dainotti, M.G.; Petrosian, V.; Singal, J.; Ostrowski, M. Determination of the Intrinsic Luminosity Time Correlation in the X-Ray Afterglows of Gamma-Ray Bursts. *The Astrophysical Journal* **2013**, *774*, 157, [arXiv:astro-ph.HE/1307.7297]. <https://doi.org/10.1088/0004-637X/774/2/157>.
199. Postnikov, S.; Dainotti, M.G.; Hernandez, X.; Capozziello, S. Nonparametric Study of the Evolution of the Cosmological Equation of State with SNeIa, BAO, and High-redshift GRBs. *The Astrophysical Journal* **2014**, *783*, 126, [arXiv:astro-ph.CO/1401.2939]. <https://doi.org/10.1088/0004-637X/783/2/126>.
200. Dainotti, M.G.; Nagataki, S.; Maeda, K.; Postnikov, S.; Pian, E. A study of gamma ray bursts with afterglow plateau phases associated with supernovae. *Astronomy and Astrophysics* **2017**, *600*, A98, [arXiv:astro-ph.HE/1612.02917]. <https://doi.org/10.1051/0004-6361/201628384>.
201. Efron, B.; Petrosian, V. A Simple Test of Independence for Truncated Data with Applications to Redshift Surveys. *The Astrophysical Journal* **1992**, *399*, 345. <https://doi.org/10.1086/171931>.
202. Dainotti, M.G.; Livermore, S.; Kann, D.A.; Li, L.; Oates, S.; Yi, S.; Zhang, B.; Gendre, B.; Cenko, B.; Fraija, N. The Optical Luminosity-Time Correlation for More than 100 Gamma-Ray Burst Afterglows. *The Astrophysical Journal* **2020**, *905*, L26, [arXiv:astro-ph.HE/2011.14493]. <https://doi.org/10.3847/2041-8213/abcda9>.
203. Levine, D.; Dainotti, M.; Zvonarek, K.J.; Fraija, N.; Warren, D.C.; Chandra, P.; Lloyd-Ronning, N. Examining Two-dimensional Luminosity-Time Correlations for Gamma-Ray Burst Radio Afterglows with VLA and ALMA. *The Astrophysical Journal* **2022**, *925*, 15, [arXiv:astro-ph.HE/2111.10428]. <https://doi.org/10.3847/1538-4357/ac4221>.
204. Dainotti, M.G.; Postnikov, S.; Hernandez, X.; Ostrowski, M. A Fundamental Plane for Long Gamma-Ray Bursts with X-Ray Plateaus. *The Astrophysical Journal* **2016**, *825*, L20, [arXiv:astro-ph.HE/1604.06840]. <https://doi.org/10.3847/2041-8205/825/2/L20>.
205. Dainotti, M.G.; Hernandez, X.; Postnikov, S.; Nagataki, S.; O'Brien, P.; Willingale, R.; Striegel, S. A Study of the Gamma-Ray Burst Fundamental Plane. *The Astrophysical Journal* **2017**, *848*, 88, [arXiv:astro-ph.HE/1704.04908]. <https://doi.org/10.3847/1538-4357/aa8a6b>.
206. Dainotti, M.G.; Lenart, A.L.; Sarracino, G.; Nagataki, S.; Capozziello, S.; Fraija, N. The X-Ray Fundamental Plane of the Platinum Sample, the Kilonovae, and the SNe Ib/c Associated with GRBs. *The Astrophysical Journal* **2020**, *904*, 97, [arXiv:astro-ph.HE/2010.02092]. <https://doi.org/10.3847/1538-4357/abbe8a>.
207. Yi, S.X.; Du, M.; Liu, T. Statistical Analyses of the Energies of X-Ray Plateaus and Flares in Gamma-Ray Bursts. *The Astrophysical Journal* **2022**, *924*, 69, [arXiv:astro-ph.HE/2111.01041]. <https://doi.org/10.3847/1538-4357/ac35e7>.
208. Cannizzo, J.K.; Gehrels, N. A New Paradigm for Gamma-ray Bursts: Long-term Accretion Rate Modulation by an External Accretion Disk. *The Astrophysical Journal* **2009**, *700*, 1047–1058, [arXiv:astro-ph.HE/0901.3564]. <https://doi.org/10.1088/0004-637X/700/2/1047>.
209. Cannizzo, J.K.; Troja, E.; Gehrels, N. Fall-back Disks in Long and Short Gamma-Ray Bursts. *The Astrophysical Journal* **2011**, *734*, 35, [arXiv:astro-ph.HE/1104.0456]. <https://doi.org/10.1088/0004-637X/734/1/35>.

210. Dai, Z.G.; Lu, T. Gamma-ray burst afterglows and evolution of postburst fireballs with energy injection from strongly magnetic millisecond pulsars. *Astronomy and Astrophysics* **1998**, *333*, L87–L90, [arXiv:astro-ph/9810402]. <https://doi.org/10.48550/arXiv.astro-ph/9810402>.
211. Dall’Osso, S.; Stratta, G.; Guetta, D.; Covino, S.; De Cesare, G.; Stella, L. Gamma-ray bursts afterglows with energy injection from a spinning down neutron star. *Astronomy and Astrophysics* **2011**, *526*, A121, [arXiv:astro-ph.HE/1004.2788]. <https://doi.org/10.1051/0004-6361/201014168>.
212. Geng, J.J.; Wu, X.F.; Huang, Y.F.; Li, L.; Dai, Z.G. Imprints of Electron-Positron Winds on the Multiwavelength Afterglows of Gamma-ray Bursts. *The Astrophysical Journal* **2016**, *825*, 107, [arXiv:astro-ph.HE/1605.01334]. <https://doi.org/10.3847/0004-637X/825/2/107>.
213. Rowlinson, A.; Gompertz, B.P.; Dainotti, M.; O’Brien, P.T.; Wijers, R.A.M.J.; van der Horst, A.J. Constraining properties of GRB magnetar central engines using the observed plateau luminosity and duration correlation. *Monthly Notices of the Royal Astronomical Society* **2014**, *443*, 1779–1787, [arXiv:astro-ph.HE/1407.1053]. <https://doi.org/10.1093/mnras/stu1277>.
214. Geng, J.J.; Wu, X.F.; Huang, Y.F.; Yu, Y.B. Delayed Energy Injection Model for Gamma-Ray Burst Afterglows. *The Astrophysical Journal* **2013**, *779*, 28, [arXiv:astro-ph.HE/1307.4517]. <https://doi.org/10.1088/0004-637X/779/1/28>.
215. Beniamini, P.; Duque, R.; Daigne, F.; Mochkovitch, R. X-ray plateaus in gamma-ray bursts’ light curves from jets viewed slightly off-axis. *Monthly Notices of the Royal Astronomical Society* **2020**, *492*, 2847–2857, [arXiv:astro-ph.HE/1907.05899]. <https://doi.org/10.1093/mnras/staa070>.
216. Beniamini, P.; Gill, R.; Granot, J. Robust features of off-axis gamma-ray burst afterglow light curves. *Monthly Notices of the Royal Astronomical Society* **2022**, *515*, 555–570, [arXiv:astro-ph.HE/2204.06008]. <https://doi.org/10.1093/mnras/stac1821>.
217. O’Connor, B.; Troja, E.; Ryan, G.; Beniamini, P.; van Eerten, H.; Granot, J.; Dichiara, S.; Ricci, R.; Lipunov, V.; Gillanders, J.H.; et al. A structured jet explains the extreme GRB 221009A. *Science Advances* **2023**, *9*, eadi1405, [arXiv:astro-ph.HE/2302.07906]. <https://doi.org/10.1126/sciadv.adi1405>.
218. Xu, M.; Huang, Y.F. New three-parameter correlation for gamma-ray bursts with a plateau phase in the afterglow. *Astronomy and Astrophysics* **2012**, *538*, A134, [arXiv:astro-ph.HE/1103.3978]. <https://doi.org/10.1051/0004-6361/201117754>.
219. Tang, C.H.; Huang, Y.F.; Geng, J.J.; Zhang, Z.B. Statistical Study of Gamma-Ray Bursts with a Plateau Phase in the X-Ray Afterglow. *The Astrophysical Journal Supplement Series* **2019**, *245*, 1, [arXiv:astro-ph.HE/1905.07929]. <https://doi.org/10.3847/1538-4365/ab4711>.
220. Deng, C.; Huang, Y.F.; Xu, F. Pseudo-redshifts of Gamma-Ray Bursts Derived from the L-T-E Correlation. *The Astrophysical Journal* **2023**, *943*, 126, [arXiv:astro-ph.HE/2212.01990]. <https://doi.org/10.3847/1538-4357/acaefd>.
221. Dai, Z.G. Relativistic Wind Bubbles and Afterglow Signatures. *The Astrophysical Journal* **2004**, *606*, 1000–1005, [arXiv:astro-ph/0308468]. <https://doi.org/10.1086/383019>.
222. Yu, Y.W.; Dai, Z.G. Shallow decay phase of GRB X-ray afterglows from relativistic wind bubbles. *Astronomy and Astrophysics* **2007**, *470*, 119–122, [arXiv:astro-ph/0705.1108]. <https://doi.org/10.1051/0004-6361:20077053>.
223. Yu, Y.W.; Liu, X.W.; Dai, Z.G. Observational Signatures of High-Energy Emission during the Shallow Decay Phase of Gamma-Ray Burst X-Ray Afterglows. *The Astrophysical Journal* **2007**, *671*, 637–644, [arXiv:astro-ph/0706.3741]. <https://doi.org/10.1086/522829>.
224. Geng, J.J.; Dai, Z.G.; Huang, Y.F.; Wu, X.F.; Li, L.B.; Li, B.; Meng, Y.Z. Brightening X-Ray/Optical/Radio Emission of GW170817/SGRB 170817A: Evidence for an Electron-Positron Wind from the Central Engine? *The Astrophysical Journal* **2018**, *856*, L33, [arXiv:astro-ph.HE/1803.07219]. <https://doi.org/10.3847/2041-8213/aab7f9>.
225. Bernardini, M.G.; Margutti, R.; Zaninoni, E.; Chincarini, G. A universal scaling for short and long gamma-ray bursts: $E_{X,iso} - E_{\gamma,iso} - E_{pk}$. *Monthly Notices of the Royal Astronomical Society* **2012**, *425*, 1199–1204, [arXiv:astro-ph.HE/1203.1060]. <https://doi.org/10.1111/j.1365-2966.2012.21487.x>.
226. Margutti, R.; Zaninoni, E.; Bernardini, M.G.; Chincarini, G.; Pasotti, F.; Guidorzi, C.; Angelini, L.; Burrows, D.N.; Capalbi, M.; Evans, P.A.; et al. The prompt-afterglow connection in gamma-ray bursts: a comprehensive statistical analysis of Swift X-ray light curves. *Monthly Notices of the Royal Astronomical Society* **2013**, *428*, 729–742, [arXiv:astro-ph.HE/1203.1059]. <https://doi.org/10.1093/mnras/sts066>.
227. Zaninoni, E.; Bernardini, M.G.; Margutti, R.; Amati, L. Update on the GRB universal scaling $E_{X,iso} - E_{\gamma,iso} - E_{pk}$ with 10 years of Swift data. *Monthly Notices of the Royal Astronomical Society* **2016**, *455*, 1375–1384, [arXiv:astro-ph.HE/1510.05673]. <https://doi.org/10.1093/mnras/stv2393>.
228. Lazzati, D.; Morsony, B.J.; Margutti, R.; Begelman, M.C. Photospheric Emission as the Dominant Radiation Mechanism in Long-duration Gamma-Ray Bursts. *The Astrophysical Journal* **2013**, *765*, 103, [arXiv:astro-ph.HE/1301.3920]. <https://doi.org/10.1088/0004-637X/765/2/103>.
229. Dado, S.; Dar, A. On the Recently Discovered Correlations between Gamma-Ray and X-Ray Properties of Gamma-Ray Bursts. *The Astrophysical Journal* **2013**, *775*, 16, [arXiv:astro-ph.HE/1203.5886]. <https://doi.org/10.1088/0004-637X/775/1/16>.
230. Izzo, L.; Muccino, M.; Zaninoni, E.; Amati, L.; Della Valle, M. New measurements of Ω_m from gamma-ray bursts. *Astronomy and Astrophysics* **2015**, *582*, A115, [arXiv:astro-ph.CO/1508.05898]. <https://doi.org/10.1051/0004-6361/201526461>.
231. Ruffini, R.; Muccino, M.; Bianco, C.L.; Enderli, M.; Izzo, L.; Kovacevic, M.; Penacchioni, A.V.; Pisani, G.B.; Rueda, J.A.; Wang, Y. On binary-driven hypernovae and their nested late X-ray emission. *Astronomy and Astrophysics* **2014**, *565*, L10, [arXiv:astro-ph.HE/1404.3946]. <https://doi.org/10.1051/0004-6361/201423812>.

232. Muccino, M.; Izzo, L.; Luongo, O.; Boshkayev, K.; Amati, L.; Della Valle, M.; Pisani, G.B.; Zaninoni, E. Tracing Dark Energy History with Gamma-Ray Bursts. *The Astrophysical Journal* **2021**, *908*, 181, [arXiv:astro-ph.CO/2012.03392]. <https://doi.org/10.3847/1538-4357/abd254>.
233. Muccino, M.; Boshkayev, K. Physical insight into the Combo-relation. *Monthly Notices of the Royal Astronomical Society* **2017**, *468*, 570–576. <https://doi.org/10.1093/mnras/stx474>.
234. Chevallier, M.; Polarski, D. Accelerating Universes with Scaling Dark Matter. *International Journal of Modern Physics D* **2001**, *10*, 213–223, [arXiv:gr-qc/gr-qc/0009008]. <https://doi.org/10.1142/S0218271801000822>.
235. Linder, E.V. Exploring the Expansion History of the Universe. *Physical Review Letters* **2003**, *90*, 091301, [arXiv:astro-ph/astro-ph/0208512]. <https://doi.org/10.1103/PhysRevLett.90.091301>.
236. Wang, J.S.; Wang, F.Y.; Cheng, K.S.; Dai, Z.G. Measuring dark energy with the $E_{iso} - E_p$ correlation of gamma-ray bursts using model-independent methods. *Astronomy and Astrophysics* **2016**, *585*, A68, [arXiv:astro-ph.HE/1509.08558]. <https://doi.org/10.1051/0004-6361/201526485>.
237. Scolnic, D.M.; Jones, D.O.; Rest, A.; Pan, Y.C.; Chornock, R.; Foley, R.J.; Huber, M.E.; Kessler, R.; Narayan, G.; Riess, A.G.; et al. The Complete Light-curve Sample of Spectroscopically Confirmed SNe Ia from Pan-STARRS1 and Cosmological Constraints from the Combined Pantheon Sample. *The Astrophysical Journal* **2018**, *859*, 101, [arXiv:astro-ph.CO/1710.00845]. <https://doi.org/10.3847/1538-4357/aab9bb>.
238. Jia, X.D.; Hu, J.P.; Yang, J.; Zhang, B.B.; Wang, F.Y. $E_{iso} - E_p$ correlation of gamma-ray bursts: calibration and cosmological applications. *Monthly Notices of the Royal Astronomical Society* **2022**, *516*, 2575–2585, [arXiv:astro-ph.HE/2208.09272]. <https://doi.org/10.1093/mnras/stac2356>.
239. Kodama, Y.; Yonetoku, D.; Murakami, T.; Tanabe, S.; Tsutsui, R.; Nakamura, T. Gamma-ray bursts in $1.8 < z < 5.6$ suggest that the time variation of the dark energy is small. *Monthly Notices of the Royal Astronomical Society* **2008**, *391*, L1–L4, [arXiv:astro-ph/0802.3428]. <https://doi.org/10.1111/j.1745-3933.2008.00508.x>.
240. Ryan, J.; Doshi, S.; Ratra, B. Constraints on dark energy dynamics and spatial curvature from Hubble parameter and baryon acoustic oscillation data. *Monthly Notices of the Royal Astronomical Society* **2018**, *480*, 759–767, [arXiv:astro-ph.CO/1805.06408]. <https://doi.org/10.1093/mnras/sty1922>.
241. Capozziello, S.; D’Agostino, R.; Luongo, O. Cosmographic analysis with Chebyshev polynomials. *Monthly Notices of the Royal Astronomical Society* **2018**, *476*, 3924–3938, [arXiv:astro-ph.CO/1712.04380]. <https://doi.org/10.1093/mnras/sty422>.
242. Yu, H.; Ratra, B.; Wang, F.Y. Hubble Parameter and Baryon Acoustic Oscillation Measurement Constraints on the Hubble Constant, the Deviation from the Spatially Flat Λ CDM Model, the Deceleration-Acceleration Transition Redshift, and Spatial Curvature. *The Astrophysical Journal* **2018**, *856*, 3, [arXiv:astro-ph.CO/1711.03437]. <https://doi.org/10.3847/1538-4357/aab0a2>.
243. Amati, L.; D’Agostino, R.; Luongo, O.; Muccino, M.; Tantalò, M. Addressing the circularity problem in the $E_p - E_{iso}$ correlation of gamma-ray bursts. *Monthly Notices of the Royal Astronomical Society* **2019**, *486*, L46–L51, [arXiv:astro-ph.HE/1811.08934]. <https://doi.org/10.1093/mnras/1811.08934>.
244. Luongo, O.; Muccino, M. A Roadmap to Gamma-Ray Bursts: New Developments and Applications to Cosmology. *Galaxies* **2021**, *9*, 77, [arXiv:astro-ph.HE/2110.14408]. <https://doi.org/10.3390/galaxies9040077>.
245. Seikel, M.; Clarkson, C.; Smith, M. Reconstruction of dark energy and expansion dynamics using Gaussian processes. *Journal of Cosmology and Astroparticle Physics* **2012**, *2012*, 036, [arXiv:astro-ph.CO/1204.2832]. <https://doi.org/10.1088/1475-7516/2012/06/036>.
246. Wang, D.Z.; Zhao, X.H.; Zhang, Z.J.; Zhang, B.B.; Peng, Z.Y. A Comprehensive Consistency Check between Synchrotron Radiation and the Observed Gamma-Ray Burst Spectra. *The Astrophysical Journal* **2022**, *926*, 178, [arXiv:astro-ph.HE/2107.09859]. <https://doi.org/10.3847/1538-4357/ac4782>.
247. Hu, J.P.; Wang, F.Y.; Dai, Z.G. Measuring cosmological parameters with a luminosity-time correlation of gamma-ray bursts. *Monthly Notices of the Royal Astronomical Society* **2021**, *507*, 730–742, [arXiv:astro-ph.CO/2107.12718]. <https://doi.org/10.1093/mnras/stab2180>.
248. Dainotti, M.G.; Amati, L. Gamma-ray Burst Prompt Correlations: Selection and Instrumental Effects. *Publications of the Astronomical Society of the Pacific* **2018**, *130*, 051001, [arXiv:astro-ph.HE/1704.00844]. <https://doi.org/10.1088/1538-3873/aaa8d7>.
249. Ghirlanda, G.; Nava, L.; Ghisellini, G. Spectral-luminosity relation within individual Fermi gamma rays bursts. *Astronomy and Astrophysics* **2010**, *511*, A43, [arXiv:astro-ph.HE/0908.2807]. <https://doi.org/10.1051/0004-6361/200913134>.
250. Khadka, N.; Ratra, B. Constraints on cosmological parameters from gamma-ray burst peak photon energy and bolometric fluence measurements and other data. *Monthly Notices of the Royal Astronomical Society* **2020**, *499*, 391–403, [arXiv:astro-ph.CO/2007.13907]. <https://doi.org/10.1093/mnras/staa2779>.
251. Khadka, N.; Luongo, O.; Muccino, M.; Ratra, B. Do gamma-ray burst measurements provide a useful test of cosmological models? *Journal of Cosmology and Astroparticle Physics* **2021**, *2021*, 042, [arXiv:astro-ph.CO/2105.12692]. <https://doi.org/10.1088/1475-7516/2021/09/042>.
252. Liu, Y.; Chen, F.; Liang, N.; Yuan, Z.; Yu, H.; Wu, P. The Improved Amati Correlations from Gaussian Copula. *The Astrophysical Journal* **2022**, *931*, 50, [arXiv:astro-ph.CO/2203.03178]. <https://doi.org/10.3847/1538-4357/ac66d3>.
253. Fana Dirirsa, F.; Razzaque, S.; Piron, F.; Arimoto, M.; Axelsson, M.; Kocevski, D.; Longo, F.; Ohno, M.; Zhu, S. Spectral Analysis of Fermi-LAT Gamma-Ray Bursts with Known Redshift and their Potential Use as Cosmological Standard Candles. *The Astrophysical Journal* **2019**, *887*, 13, [arXiv:astro-ph.HE/1910.07009]. <https://doi.org/10.3847/1538-4357/ab4e11>.

254. Cao, S.; Ratra, B. Testing the standardizability of, and deriving cosmological constraints from, a new Amati-correlated gamma-ray burst data compilation. *Journal of Cosmology and Astroparticle Physics* **2024**, *2024*, 093, [arXiv:astro-ph.CO/2404.08697]. <https://doi.org/10.1088/1475-7516/2024/10/093>.
255. Cao, S.; Ratra, B. $H_0=69.8 \pm 1.3 \text{ km s}^{-1} \text{ Mpc}^{-1}$, $\Omega_{m0}=0.288 \pm 0.017$, and other constraints from lower-redshift, non-CMB, expansion-rate data. *Physical Review D* **2023**, *107*, 103521, [arXiv:astro-ph.CO/2302.14203]. <https://doi.org/10.1103/PhysRevD.107.103521>.
256. Cao, S.; Ryan, J.; Khadka, N.; Ratra, B. Cosmological constraints from higher redshift gamma-ray burst, H II starburst galaxy, and quasar (and other) data. *Monthly Notices of the Royal Astronomical Society* **2021**, *501*, 1520–1538, [arXiv:astro-ph.CO/2009.12953]. <https://doi.org/10.1093/mnras/staa3748>.
257. Cao, S.; Ratra, B. Using lower redshift, non-CMB, data to constrain the Hubble constant and other cosmological parameters. *Monthly Notices of the Royal Astronomical Society* **2022**, *513*, 5686–5700, [arXiv:astro-ph.CO/2203.10825]. <https://doi.org/10.1093/mnras/stac1184>.
258. Tsutsui, R.; Nakamura, T.; Yonetoku, D.; Murakami, T.; Kodama, Y.; Takahashi, K. Cosmological constraints from calibrated Yonetoku and Amati relation suggest fundamental plane of gamma-ray bursts. *Journal of Cosmology and Astroparticle Physics* **2009**, *2009*, 015, [arXiv:astro-ph/0810.1870]. <https://doi.org/10.1088/1475-7516/2009/08/015>.
259. Tsutsui, R.; Nakamura, T.; Yonetoku, D.; Murakami, T.; Tanabe, S.; Kodama, Y.; Takahashi, K. Constraints on w_0 and w_a of dark energy from high-redshift gamma-ray bursts. *Monthly Notices of the Royal Astronomical Society* **2009**, *394*, L31–L35, [arXiv:astro-ph/0807.2911]. <https://doi.org/10.1111/j.1745-3933.2008.00604.x>.
260. Tian, X.; Li, J.L.; Yi, S.X.; Yang, Y.P.; Hu, J.P.; Qu, Y.K.; Wang, F.Y. Radio Plateaus in Gamma-Ray Burst Afterglows and Their Application in Cosmology. *The Astrophysical Journal* **2023**, *958*, 74, [arXiv:astro-ph.HE/2310.00596]. <https://doi.org/10.3847/1538-4357/acfd8>.
261. Li, J.L.; Yang, Y.P.; Yi, S.X.; Hu, J.P.; Qu, Y.K.; Wang, F.Y. Standardizing the gamma-ray burst as a standard candle and applying it to cosmological probes: Constraints on the two-component dark energy model. *Astronomy and Astrophysics* **2024**, *689*, A165, [arXiv:astro-ph.HE/2405.17010]. <https://doi.org/10.1051/0004-6361/202348542>.
262. Cao, S.; Khadka, N.; Ratra, B. Standardizing Dainotti-correlated gamma-ray bursts, and using them with standardized Amati-correlated gamma-ray bursts to constrain cosmological model parameters. *Monthly Notices of the Royal Astronomical Society* **2022**, *510*, 2928–2947, [arXiv:astro-ph.CO/2110.14840]. <https://doi.org/10.1093/mnras/stab3559>.
263. Cao, S.; Dainotti, M.; Ratra, B. Standardizing Platinum Dainotti-correlated gamma-ray bursts, and using them with standardized Amati-correlated gamma-ray bursts to constrain cosmological model parameters. *Monthly Notices of the Royal Astronomical Society* **2022**, *512*, 439–454, [arXiv:astro-ph.CO/2201.05245]. <https://doi.org/10.1093/mnras/stac517>.
264. Cao, S.; Dainotti, M.; Ratra, B. Gamma-ray burst data strongly favour the three-parameter fundamental plane (Dainotti) correlation over the two-parameter one. *Monthly Notices of the Royal Astronomical Society* **2022**, *516*, 1386–1405, [arXiv:astro-ph.CO/2204.08710]. <https://doi.org/10.1093/mnras/stac2170>.
265. Xu, F.; Tang, C.H.; Geng, J.J.; Wang, F.Y.; Wang, Y.Y.; Kuerban, A.; Huang, Y.F. X-Ray Plateaus in Gamma-Ray Burst Afterglows and Their Application in Cosmology. *The Astrophysical Journal* **2021**, *920*, 135, [arXiv:astro-ph.HE/2012.05627]. <https://doi.org/10.3847/1538-4357/ac158a>.
266. Riess, A.G.; Casertano, S.; Yuan, W.; Macri, L.M.; Scolnic, D. Large Magellanic Cloud Cepheid Standards Provide a 1% Foundation for the Determination of the Hubble Constant and Stronger Evidence for Physics beyond Λ CDM. *The Astrophysical Journal* **2019**, *876*, 85, [arXiv:astro-ph.CO/1903.07603]. <https://doi.org/10.3847/1538-4357/ab1422>.
267. Planck Collaboration.; Aghanim, N.; Akrami, Y.; Ashdown, M.; Aumont, J.; Baccigalupi, C.; Ballardini, M.; Banday, A.J.; Barreiro, R.B.; Bartolo, N.; et al. Planck 2018 results. VI. Cosmological parameters. *Astronomy and Astrophysics* **2020**, *641*, A6, [arXiv:astro-ph.CO/1807.06209]. <https://doi.org/10.1051/0004-6361/201833910>.
268. Atteia, J.L. A simple empirical redshift indicator for gamma-ray bursts. *Astronomy and Astrophysics* **2003**, *407*, L1–L4, [arXiv:astro-ph/0304327]. <https://doi.org/10.1051/0004-6361:20030958>.
269. Dainotti, M.G.; Fabrizio Cardone, V.; Capozziello, S.; Ostrowski, M.; Willingale, R. Study of Possible Systematics in the $L^*_X-T^*_a$ Correlation of Gamma-ray Bursts. *The Astrophysical Journal* **2011**, *730*, 135, [arXiv:astro-ph.HE/1101.1676]. <https://doi.org/10.1088/0004-637X/730/2/135>.
270. Dainotti, M.G.; Narendra, A.; Pollo, A.; Petrosian, V.; Bogdan, M.; Iwasaki, K.; Prochaska, J.X.; Rinaldi, E.; Zhou, D. Gamma-Ray Bursts as Distance Indicators by a Statistical Learning Approach. *The Astrophysical Journal* **2024**, *967*, L30, [arXiv:astro-ph.HE/2402.04551]. <https://doi.org/10.3847/2041-8213/ad4970>.
271. Bargiacchi, G.; Dainotti, M.G.; Capozziello, S. High-redshift Cosmology by Gamma-Ray Bursts: an overview. *arXiv e-prints* **2024**, p. arXiv:2408.10707, [arXiv:astro-ph.CO/2408.10707]. <https://doi.org/10.48550/arXiv.2408.10707>.
272. Aldowma, T.; Razzaque, S. Deep Neural Networks for estimation of gamma-ray burst redshifts. *Monthly Notices of the Royal Astronomical Society* **2024**, *529*, 2676–2685, [arXiv:astro-ph.HE/2401.11005]. <https://doi.org/10.1093/mnras/stae535>.
273. Narendra, A.; Dainotti, M.; Sarkar, M.; Lenart, A.; Bogdan, M.; Pollo, A.; Zhang, B.; Rabeda, A.; Petrosian, V.; Kazunari, I. GRB Redshift Estimation using Machine Learning and the Associated Web-App. *arXiv e-prints* **2024**, p. arXiv:2410.13985, [arXiv:astro-ph.HE/2410.13985]. <https://doi.org/10.48550/arXiv.2410.13985>.

274. Wei, J.; Cordier, B.; Antier, S.; Antilogus, P.; Atteia, J.L.; Bajat, A.; Basa, S.; Beckmann, V.; Bernardini, M.G.; Boissier, S.; et al. The Deep and Transient Universe in the SVOM Era: New Challenges and Opportunities - Scientific prospects of the SVOM mission. *arXiv e-prints* **2016**, p. arXiv:1610.06892, [arXiv:astro-ph.IM/1610.06892]. <https://doi.org/10.48550/arXiv.1610.06892>.
275. Yuan, W.; Zhang, C.; Feng, H.; Zhang, S.N.; Ling, Z.X.; Zhao, D.; Deng, J.; Qiu, Y.; Osborne, J.P.; O'Brien, P.; et al. Einstein Probe - a small mission to monitor and explore the dynamic X-ray Universe. *arXiv e-prints* **2015**, p. arXiv:1506.07735, [arXiv:astro-ph.HE/1506.07735]. <https://doi.org/10.48550/arXiv.1506.07735>.
276. Amati, L.; O'Brien, P.; Götz, D.; Bozzo, E.; Tenzer, C.; Frontera, F.; Ghirlanda, G.; Labanti, C.; Osborne, J.P.; Stratta, G.; et al. The THESEUS space mission concept: science case, design and expected performances. *Advances in Space Research* **2018**, *62*, 191–244, [arXiv:astro-ph.IM/1710.04638]. <https://doi.org/10.1016/j.asr.2018.03.010>.
277. Hu, J.P.; Wang, F.Y. Hubble Tension: The Evidence of New Physics. *Universe* **2023**, *9*, 94, [arXiv:astro-ph.CO/2302.05709]. <https://doi.org/10.3390/universe9020094>.

Disclaimer/Publisher's Note: The statements, opinions and data contained in all publications are solely those of the individual author(s) and contributor(s) and not of MDPI and/or the editor(s). MDPI and/or the editor(s) disclaim responsibility for any injury to people or property resulting from any ideas, methods, instructions or products referred to in the content.